

https://dspace.org/

The impact of seawater diversion into an Estuarine System, St. Lucia, South Africa

Loonat, Muhammad

2022

https://hdl.handle.net/10539/33856

Downloaded from a DSpace repository. https://dspace.org/

UNIVERSITY OF THE WITWATERSRAND, JOHANNESBURG

The Impact of Seawater Diversion into an Estuarine System, St. Lucia, South Africa

By:

Muhammad Loonat

1429871

Supervisor: Prof. T. Abiye

A research report submitted in partial fulfilment of the requirements for the degree of Master of Science in Hydrogeology

27 January 2022

School of Geosciences

University of the Witwatersrand

NRF National Research Foundation

DECLARATION

I, **Muhammad Loonat**, Student number: **1429871**, am a student registered for **GEOL7028A** in the year **2021**. I hereby declare the following:

I am aware that plagiarism (the use of someone else's work without their permission and/or without acknowledging the original source) is wrong.

I confirm that the work submitted for assessment for the above course is my own unaided work explicitly where I have indicated otherwise.

I understand that the University of the Witwatersrand may take disciplinary action against me if there is a belief that this is not my own unaided work or that I have failed to acknowledge the source of the ideas or words in my writing.

Signature:

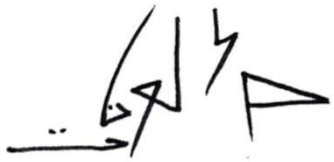

Date: 27 January 2022

ABSTRACT

Coastal aquifers such as the unconfined aquifer in St. Lucia, KwaZulu-Natal, South Africa, are susceptible to seawater intrusion which may be exacerbated by the impacts of climate change and increasing coastal populations. Residents and businesses are largely dependent on groundwater for daily use due to poor municipal water supply. To determine whether fresh groundwater was being contaminated through mixing with seawater, groundwater samples were collected from boreholes in the St. Lucia town and Khula and Duku villages further inland. Physicochemical, hydrochemical and stable water isotope analyses ($\delta^{2}H$ and $\delta^{18}O$) were conducted on a total of 52 samples collected from the sea, estuary, river and groundwater in January and February 2021. The stable isotope analysis was conducted at the WITS Hydrogeology Laboratory while the hydrochemical analyses were outsourced to an external SANAS accredited laboratory in Pretoria. The results showed that for most samples, low electrical conductivity (EC) values combined with low Cl/Br ratios and isotopic mixing proportions closer to that of fresh groundwater, indicate that seawater intrusion did not occur to a great extent within the uppermost water-bearing hydrostratigraphic unit (HSU). This HSU is composed of sands, clays, and silts, and remains the primary unit from which groundwater is abstracted. The position of the Cretaceous aquiclude below the water-bearing HSU, seaward flow of groundwater and estuary-produced freshwater lens serve as important buffers for the inland advancement of seawater as conceptualised in a seawater interface model. Two groups of groundwater were determined using a Piper plot and confirmed with an agglomerative hierarchical clustering analysis (HCA) which indicates that different processes are at play to produce each group. Group 1 waters are of Na-Cl type which have likely undergone recycling through evaporation, infiltration, and precipitation, while group 2 waters are of Ca-HCO_3+CO_3 type with the calcarenites of the Uloa Fm and calcareously cemented dune sands of the Kosi Bay Fm being possible source aquifers. Some samples exhibit hydrochemical or isotopic signatures close to that of seawater indicating minor mixing due to high rates of groundwater abstraction and concentration of Cl, Mg and Na by evaporation, septic tank waste, animal waste and agricultural return flows. Groundwater within the study area is considered largely uncontaminated by seawater intrusion, however, continuous monitoring of water levels and physicochemical variables is advised to prevent seawater intrusion in the future and maintain or improve the current groundwater quality.

ACKNOWLEDGEMENTS

Firstly, I would like to thank the Almighty for blessing me with the life, health, and ability to conduct my research.

I also extend my gratitude to my beloved parents and my family for their support during all my years as a student, before and beyond.

A special thanks goes to my supervisor Prof. T. Abiye for his guidance, knowledge, use of his lab and quick email responses.

I sincerely thank my friend and colleague Brad Frazer for his help and company in the field and beyond.

A hearty thanks goes to Petrus Viviers of St. Lucia and Sibusiso Mthembu of Khula Village whose insight and hospitality made my research a wonder.

I also thank Sue Van Rensberg, Paul Gordijn and Siphiwe Mfeka from the South African Environment Observation Network (SAEON) for their assistance in providing me with data to complete this project.

The research conducted here is also partly supported by the grant provided by the National Research Foundation (NRF) of South Africa (Grant number 130553).

CONTENTS

List of Figures……..Pg. vii
List of Tables……Pg. viii
List of Appendices……Pg. viii
List of Abbreviations……Pg. ix

1. INTRODUCTION…….Pg. 1
2. STUDY AREA AND LITERATURE REVIEW……. Pg. 2
   2.1 Study Area…….. Pg. 2
   2.2 Climatic and Hydrological Setting…….. Pg. 4
   2.3 Geological and Hydrogeological Setting……..… Pg. 6
3. AIMS AND OBJECTIVES…….…. Pg. 9
4. RESEARCH DESIGN AND METHODOLOGY…… Pg. 9
   4.1 Field Work…….. Pg. 9
      4.1.1 Sampling and Sampling Points……. Pg. 10
   4.2 Hydrochemical Analysis…….……..… Pg. 11
   4.3 Environmental Isotope Analysis…….……..… Pg. 12
5. RESULTS AND DISCUSSION…….…….…. Pg. 14
   5.1 Physicochemical Parameters…….…..……..Pg. 14
   5.2 Hydrochemistry……..…….…….....……...……Pg. 15
   5.3 Environmental Isotopes (^{18}O and ^{2}H) ……..…….…….....Pg. 18
   5.4 Seawater Intrusion Detection……..……..…….…….....Pg. 19
      5.4.1 Electrical Conductivity Analysis…….……..…..Pg. 19
      5.4.2 Water Sample Clustering…….…..…..Pg. 20
      5.4.3 Ionic Ratio Analysis…….……..….Pg. 23
      5.4.4 Cl/Br Ratios……..…...Pg. 26
      5.4.5 Environmental Isotope Analysis ……...…….….Pg. 27
      5.4.6 Water Mixing Proportions Using $\delta^{2}H$ and $\delta^{18}O$ ……..... Pg. 31
   5.5 Groundwater Hydrodynamics ……...…..Pg. 34
      5.5.1 Seawater Interface Conceptual Model……..….. Pg. 34
6. CONCLUSION……...…..… Pg. 38
7. RESEARCH LIMITATIONS AND RECOMMENDATIONS……..……..…. Pg. 39
8. REFERENCES…….....…. Pg. 41
9. APPENDICES……..…. Pg. 48

LIST OF FIGURES

Figure 1 – Map showing study area with points of interest and colour coded water sampling points. (Pg. 2)

Figure 2 – Average monthly rainfall for Oct 2019 - Sep 2021 from the St. Lucia town rainfall monitoring station. Data obtained from SAEON (2021). (Pg. 5)

Figure 3 – Photograph looking SW showing triple point confluence between the Mfolozi River, the estuary mouth leading to the ocean and the estuary leading to Lake St. Lucia. (Pg. 5)

Figure 4 – Map showing elevation of the study area with sampling points. (Pg. 6)

Figure 5 – A) Simplified geological map of the study area and surrounds. B) Surface cover map of the study area and surrounds. C) Simplified geological cross-section of near-surface geology adapted from Taylor *et al*., 2006 and Botha *et al*., 2013. Section line indicated in Figure 5A. (Pg. 8)

Figure 6 – The barometrically corrected water level at Hippo Well for 15 months. Data courtesy of SAEON (2021). (Pg. 15)

Figure 7 – Schoeller plot showing concentrations of major anions and cations for selected samples. (Pg. 16)

Figure 8 – Stiff diagrams for selected samples showing ion concentrations in meq/L as well as water type. (Pg. 17)

Figure 9 – Map showing ramped EC values for all samples collected with the seawater sample being the highest and groundwater samples below 1000 µS/cm. (Pg. 19)

Figure 10 – Piper (1944) plot showing two distinct water groups. Group 1 of Na-Cl type and Group 2 of Ca-HCO_3+CO_3 type. (Pg. 21)

Figure 11 – Satellite image showing the locations of selected sampling points with group 1 samples in yellow and group 2 samples in red (Google Earth, 2021). (Pg. 22)

Figure 12 – The δ^2H and $\delta^{18}O$ values of selected samples shown by water group. (Pg. 22)

Figure 13 – Dendrogram showing water groups 1 (yellow) and 2 (red) and the dissimilarity between samples and groups due to two sets of processes occurring within the aquifer. (Pg. 23)

Figure 14 – The Mg/Ca ratios for selected samples plotted against Cl concentration shows low correlation. (Pg. 24)

Figure 15 – The Ca/SO_4 ratio plotted against TDS shows low correlation. (Pg. 25)

Figure 16 – The Cl/Br ratios for selected samples plotted against the distance from the shoreline. (Pg. 26)

Figure 17 – The $\delta^{18}O$ and $\delta^{2}H$ plotted against the KZN LMWL and the GMWL. (Pg. 29)

Figure 18 – The colour coded $\delta^{18}O$ and $\delta^{2}H$ values of selected samples plotted against the KZN LMWL and the GMWL. (Pg. 29)

Figure 19 – The $\delta^{18}O$ vs Cl concentration indicating a moderately low correlation. (Pg. 30)

Figure 20 – The $\delta^{2}H$ vs Cl concentration indicating a low correlation. (Pg. 30)

Figure 21 – The theoretical $\delta^{18}O$ and $\delta^{2}H$ values plotted against the mixing line between seawater and fresh groundwater end members. (Pg. 33)

Figure 22 – Concentrations of Na vs Cl in meq/L are plotted along the trendline that shows samples preferentially plot closer to the fresh groundwater end member. (Pg. 33)

Figure 23 – Model showing the seawater interface at depth within the uppermost aquifer where *Zs* is the seawater interface depth and *Zf* is the water table altitude. Adapted and modified from Hiscock and Bense (2014). (Pg. 37)

Figure 24 – Model showing the interaction between fresh groundwater and seawater with the unconfined water-bearing HSU, estuary freshwater lens, Cretaceous aquiclude and Port Durnford aquitard. (Pg. 37)

LIST OF TABLES

Table 1 – Standards used for the calibration of $\delta^{18}O$ and $\delta^{2}H$. (Pg. 13)

Table 2 – Hydrochemical data for selected samples. (Pg. 16)

Table 3 – Categorized min, max and average $\delta^{18}O$ and $\delta^{2}H$ values. (Pg. 18)

Table 4 – Multiple ionic ratio analyses indicating low potential for seawater intrusion. (Pg. 25)

LIST OF APPENNDICES

Appendix A – Sampling points with field data. (Pg. 49)

Appendix B – $\delta^{2}H$ (‰) values for all samples. (Pg. 50)

Appendix C – $\delta^{18}O$ (‰) values for all samples. (Pg. 52)

LIST OF ABBREVIATIONS

^{18}O – Oxygen 18

^{2}H – Hydrogen 2 (Deuterium)

a.s.l – Above Sea Level

CBE – Charge Balance Error

DEM – Digital Elevation Model

DI – Deionized Water

DKV – Duku Village Groundwater Sample

DWS – Department of Water and Sanitation

EC – Electrical Conductivity

EST – Estuary Surface Water Sample

GMWL – Global Meteoric Water Line

HSU - Hydrostratigraphic Unit

k – Hydraulic Conductivity

KLV – Khula Village Groundwater Sample

KZN – KwaZulu-Natal Province

LMWL – Local Meteoric Water Line

MWL – Meteoric Water Line

n – Porosity (Total)

ne – Porosity (Effective)

OCN – Ocean Surface Water (Seawater) Sample

pH – Potential of Hydrogen

STL – St. Lucia Town Groundwater Sample

TDS – Total Dissolved Solids

UMF – Mfolozi River Surface Water Sample

1. INTRODUCTION

An increasing urgency for the conservation of available freshwater resources in South Africa and across the globe is paramount to attaining and uplifting the right to access to clean water and sanitation. South Africa relies predominantly on surface water for domestic, industrial, and agricultural use, while only some households, rural areas and farms are supplied by groundwater (WWF-SA, 2016). It is imperative to understand groundwater as a resource since it forms an important source of freshwater for sustaining the current and future increases in water demand. Globally, surface water (lakes and rivers, etc.) accounts for approximately 0.01% of all water on Earth, while groundwater constitutes over one hundred times the volume of surface water at approximately 1.11% (White, 2018) and 29.9% of Earth's freshwater (Mook, 2000). Some areas have high dependencies on groundwater which may be compromised by the effects of climate change (Sherif and Singh, 1999) and other anthropogenic activities such as groundwater overexploitation and land-use changes (Chrystal, 2013). Recent years have seen changes in population due to both growth and urban migration which must be accounted for when managing freshwater resources (Falkenmark and Widstrand, 1992). Along the coast, freshwater aquifers are at risk of contamination by the intrusion of saline water which reduces the quality of groundwater and limits its use (Werner *et al.*, 2013). The mixing of fresh groundwater and seawater may be caused by several factors both above and beneath the surface which are investigated within this research report.

The coastal town of St. Lucia and its surrounding residential areas, the Khula and Duku Villages, are located in KwaZulu-Natal (KZN), South Africa, and rely on groundwater on a daily basis due to the limited infrastructure for the municipal water supply. The key research question is whether seawater intrusion is occurring in the study area, while the objectives focus on the extent and mechanisms of mixing, as well as groundwater chemistry and movement. Sections of the area being investigated form part of the iSimangaliso Wetlands Park (IWP) and houses a large estuary, wetland, and river (Figure 1) that is home to a variety of plant and animal species, including some of which are on the IUCN Red List (Vrdoljak and Hart, 2007). The estuary and coastline serve as a major means of income for many residents through tourism, fishing and other recreational activities amounting to over a quarter of a billion Rand in total profits (Nunes *et al.*, 2018). The estuary mouth has recently become a contentious issue as a result of its artificial opening in January 2021 after being mostly cut off from the ocean since March 2007. This has brought about renewed interest in the region for both tourists and researchers alike in terms of natural beauty and scientific allure. It is for this reason, as well as the importance of available usable groundwater for residents which has led to this research being undertaken to understand the potential impact of seawater intrusion within the area.

2. STUDY AREA & LITERATURE REVIEW

2.1 – Study Area

The iSimangaliso Wetland Park is considered a World Heritage Site declared by UNESCO (United Nations Educational, Scientific and Cultural Organization) in 1999 (IWP, 2011) and hosts four RAMSAR (Convention on Wetlands of International Importance) wetland sites within the park (IWP annual report 2019-2020). According to Whitfield and Taylor (2009), the St. Lucia estuary is one of the oldest estuaries which has been given protected status and is likely the most researched estuary in South Africa as it accounts for over half of the country's estuarine surface area (Nunes, 2019). It is no secret that the intrinsic beauty of the fauna and flora in St. Lucia coupled with its plethora of hydrological systems and rich history of anthropogenic interference poses an attractive site to conduct research within a multitude of faculties. The study area as seen in Figure 1 can be grouped into three regions: St. Lucia town, Khula Village and Duku Village.

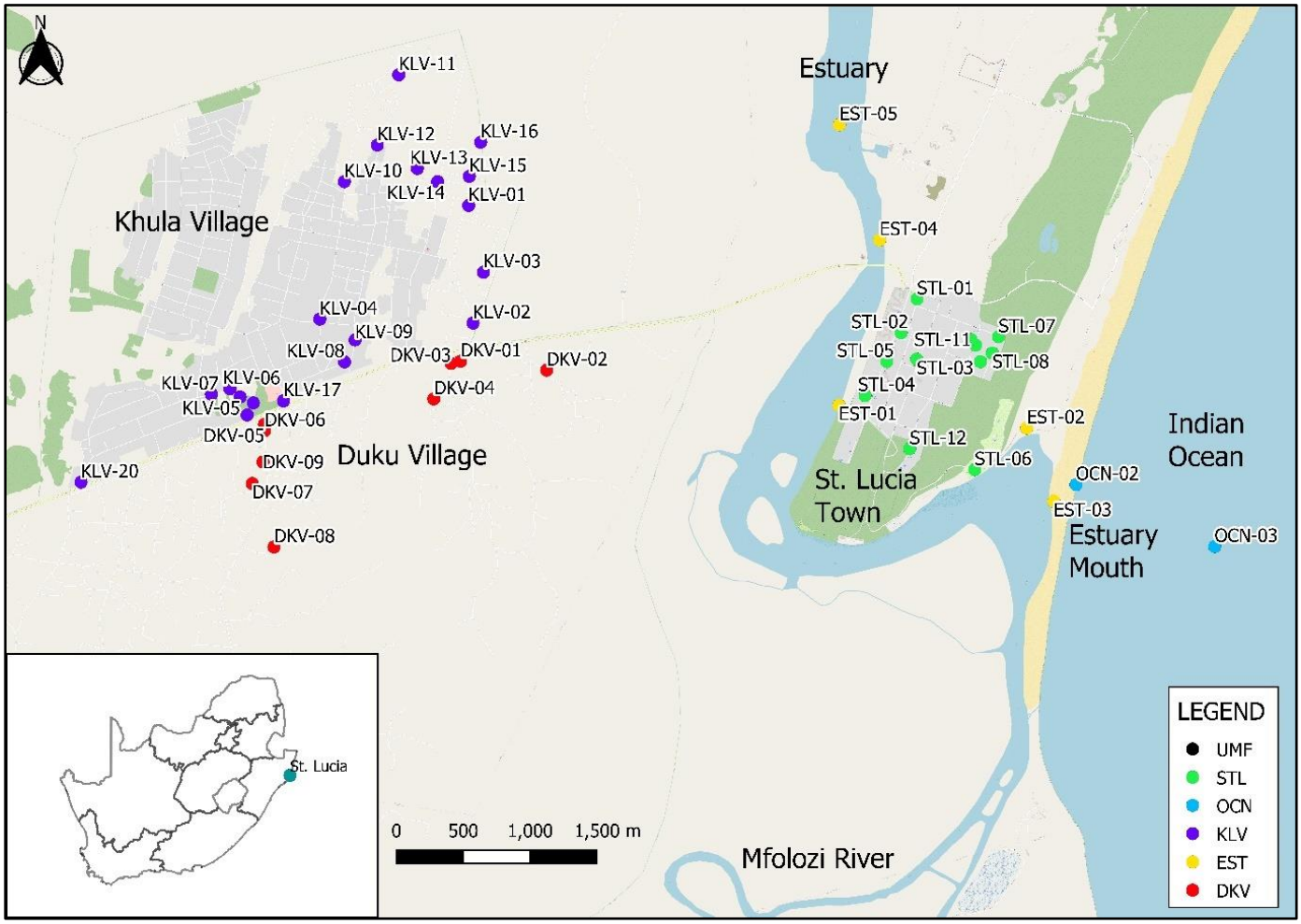

Figure 1 - Map showing the study area with points of interest and colour coded water sampling points.

Groundwater in the region is utilised locally in the St. Lucia town as well as the Khula and Duku villages located further west from the coastline. Adding complexity to the local groundwater and surface water regime is the presence of the estuary of which the first 14 km from the mouth (Taylor *et al*., 2006) is influenced by both the M2 and S2 diurnal tides (Rautenbach *et al*., 2019). The water within the estuary can be seen exhibiting bidirectional flow during the flood and ebb tides. Fresh groundwater in coastal areas, due to its proximity to the coastline, has the potential to mix with seawater, however, sections of the aquifer close to the estuary may exhibit waters with decreased salinity as a result of several local physical and chemical factors (Thibault, 2017). According to Meyer *et al.* (2001), seawater intrusion is considered unlikely across the Maputaland coastal plain due to the water table that lies above sea level. This was somewhat confirmed by Bjørkenes *et al.* (2006) who stated that the water along the eastern shores, between the estuary and ocean, has low electrical conductivity (EC) and is untainted by anthropogenic activities. Due to increased abstractions in the villages and sugarcane farms further inland, and the possibility of other factors, such as the open state of the estuary mouth, playing some role in modifying water movement within the aquifer, it begs the question of whether these statements remain true, and the fresh groundwater remains uncontaminated by saline seawater.

Both climate variability and climate change play a role in the dynamics of coastal aquifers due to periods of flooding, droughts, sea-level rise, precipitation, runoff, evapotranspiration, and fluctuations in temperature (Sherif and Singh, 1999). In this case, the sensitive estuarine system which is the largest in Africa (Gordon *et al*., 2016) is fed by groundwater, precipitation, and channel flow from rivers during the wet season (Bate *et al*., 2011; Nunes *et al*., 2017; Nunes *et al*., 2019). Anthropogenic activities which directly utilise groundwater is argued to have an even greater impact than the anthropogenically induced climate change effects (Loáiciga, 2003). This is substantiated by Været *et al*. (2009) who stated that management practices at a local scale have greater implications for groundwater than future climate change impacts.

Seawater intrusion is a common phenomenon in coastal areas around the world, with some sections of the coastline exhibiting characteristics, which facilitate the advancement of seawater into fresh groundwater more than others. Historically, early settlements along the coast in countries such as the USA were formed in areas conducive to the building of ports such as natural lagoons and deep bays (Bear *et al.*, 1999). Ironically, some of these areas were also rich in fresh groundwater resources and hence due to the increased anthropogenic activities, seawater intrusion posed a threat to groundwater and was detected as early as the year 1824 (Bear *et al.*, 1999). By the early 20th century, seawater intrusion had been well understood and Brown (1925) stated that pumping water from a well near the coast in excess to what is fed to the well will result in seawater being drawn in, with the only remedy being to abandon the well. Some of these fundamentals are still valid at the present time as is stated in

later sections of this paper. Modern geophysical methods such as the use of resistivity and electromagnetics may be employed to aid in seawater intrusion studies (Werner *et al.*, 2013). Geophysical methods, although costly, may prove useful for research into seawater intrusion in the future, along with numerical modelling, such as variable density models that predict the position of the seawater interface which can then be compared to salinity data in the field (Naik, 2018). In the case of sea-level rise, various studies have shown that an increase in sea-level by a mere 0.5 m in the Mediterranean Sea and the Bay of Bengal will potentially result in 9 km of lateral seawater intrusion into the Nile Delta aquifer in Egypt and a 0.4 km intrusion in the Madras aquifer in India, respectively (Sherif and Singh, 1999). Globally, a projected rate of sea-level rise of up to 5 mm/yr has been estimated which results in up to 0.5 m of sea-level rise by the year 2100 (Maro, 2012). The environmental and anthropogenic impacts of this could prove devastating for the conservation of fresh groundwater reserves along the world's coastlines.

2.2 – Climatic and Hydrological Setting

The study area is located along the coastline of the Indian Ocean where the Agulhas Current is dominant and exhibits ocean waters with surface temperatures from 23 °C in the winter season to as much as 28 °C in the summer (Connell and Porter, 2013; Morris *et al.*, 2013). The mean annual rainfall within the study area is calculated as 1270.87 mm based on two years of data obtained from a SAEON (South African Environmental Observation Network) rainfall monitoring station located in the St. Lucia town (-28.382767, 32.412087), close to where sample STL-12 was taken (SAEON, 2021). The SAEON rainfall values are close to the rainfall values from Adams (2021) with a stated mean annual rainfall of between 1000 mm to 1100 mm. Figure 2 shows the average monthly rainfall from Oct 2019 to Sep 2021 (SAEON, 2021). Potential Evapotranspiration (PET) varies from 3.2 mm/day to 6 mm/day (with an annual value of 1168 mm to 2190 mm) and the annual actual evapotranspiration (AET) is 900 mm (Clulow *et al.*, 2012). Summer thunderstorms occur between October and March while the winter months (April - September) are affected by mid-latitude cyclones (Nunes *et al.*, 2017). Salinity within the part of the ocean close to the continent is known to decrease during the rainy season due to increased freshwater flow from river mouths along the coast (Schumann, 1998). The area exhibits undulating topography owed to the high rates of weathering and erosion of the soft dune sands and has a maximum altitude of approximately 60 m (Figure 4).

The Indian Ocean, Mfolozi River, and estuary, which meet at a triple point confluence (Figure 3), play important roles in the area's hydrology and hydrogeology. Changes in both climate and land-use are known to shift the rates of infiltration and runoff, and therefore, must be accounted for in the implementation of any Integrated Water Resource Management (IWRM) strategies (Maro, 2012).

Within the Mfolozi catchment, less than 1% of land use accounts for urban structures while most of the land use (67%) is undisturbed and considered natural land cover (Stretch and Maro, 2013).

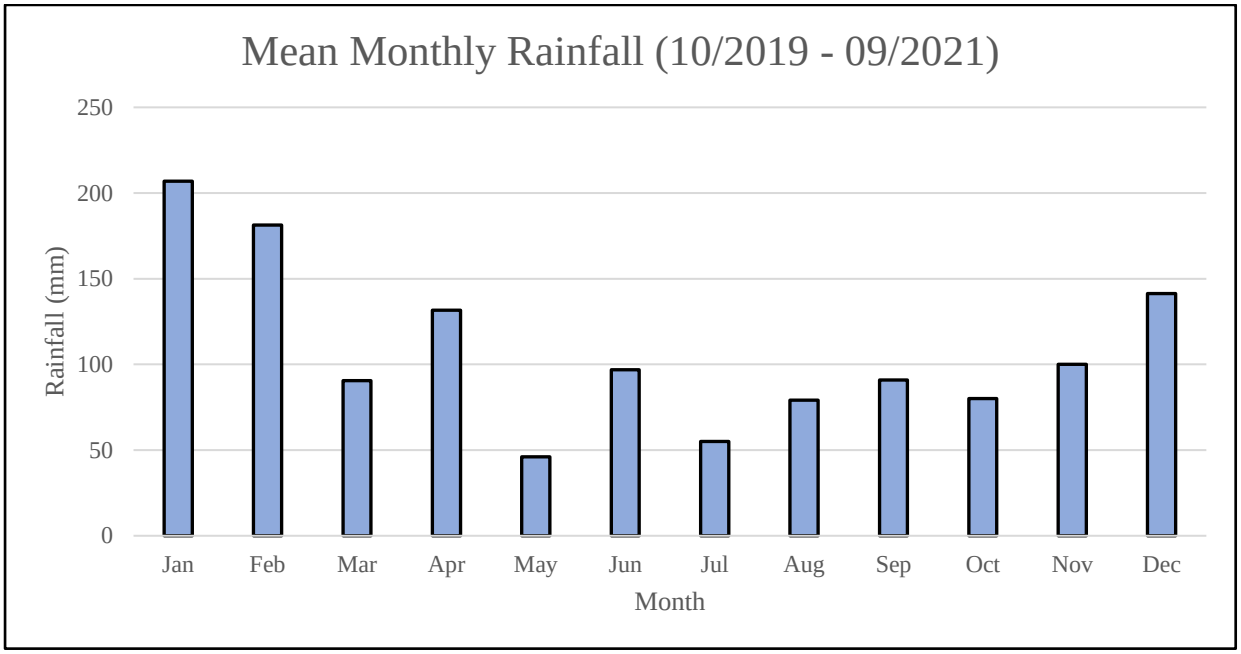

Figure 2 – Average monthly rainfall for Oct 2019 - Sep 2021 from the St. Lucia town rainfall monitoring station. Data obtained from SAEON (2021).



Figure 3 - Photograph looking SW shows the triple point confluence between the Mfolozi River, the estuary mouth leading to the ocean and the estuary leading to Lake St. Lucia.

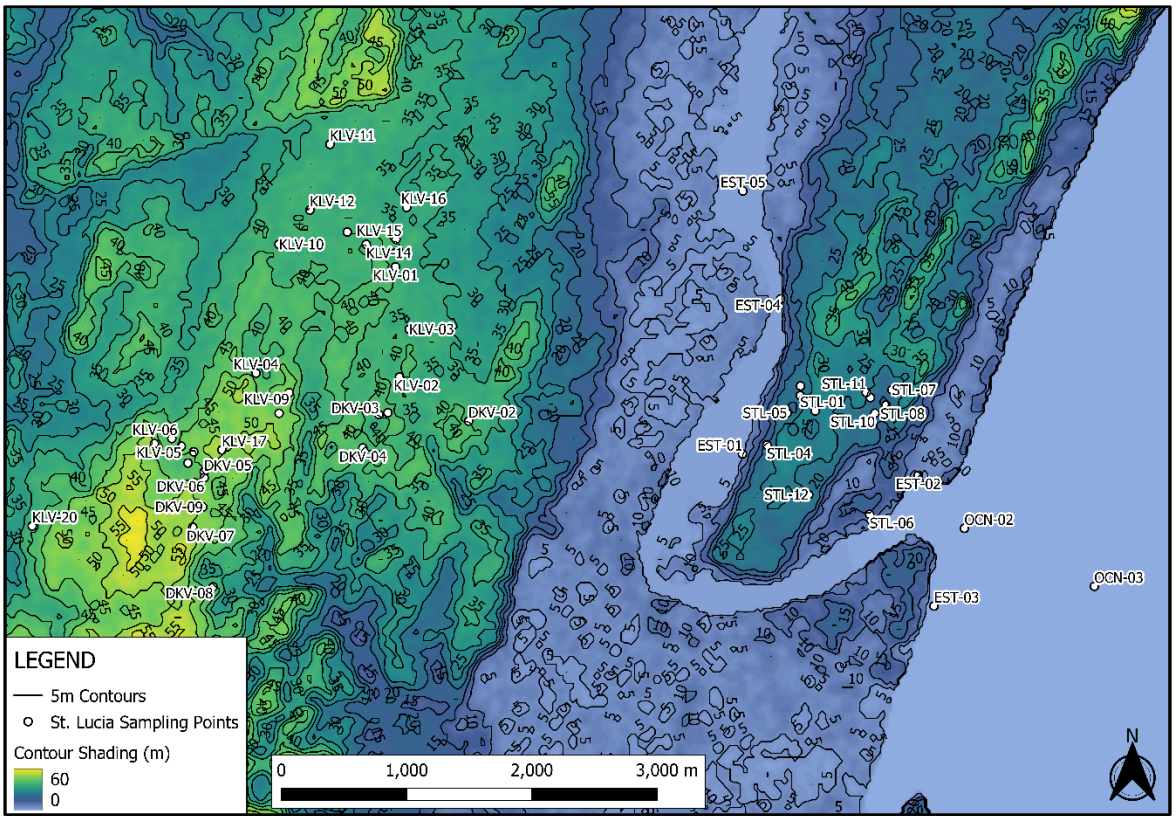

Figure 4 - Map showing the elevation of the study area with sampling points.

2.3 – Geological and Hydrogeological Setting

The study area forms part of the Maputaland coastal plain where the wetlands, lagoons and estuaries are owed to an extensive barrier dune along the coastline of the Indian Ocean (Taylor *et al.*, 2006). The geological configuration, up to approximately 1000 m depth (Kelbe *et al.*, 2013), is rather simple in contrast to the geology of other coastal areas in South Africa (McCarthy and Rubidge, 2005). Towards the west in the catchment areas which drain the Mkhuze, Msunduzi, Mzinene, Hluhluwe and Nyalazi Rivers, the Ecca Group of the Karoo Supergroup serves as a basement (Kelbe *et al.*, 2013). The Ecca Group is then overlain by the Letaba, Jozini and Movene Formations (Fms) of the Lebombo Group which are also part of the Karoo Supergroup (Kelbe *et al.*, 2013). These formations consist of basalt in the Letaba Fm and rhyolite in both the Jozini and Movene Fms and host a number of faults as seen in Figure 5A (Cleverly and Bristow, 1979). The sequence is followed by the Makatini and Mzinene Fms of the Zululand Group that are composed of sandstone with conglomerate and sandstone with marine siltstone (Kelbe *et al.*, 2013). According to Kelbe *et al.* (2013), the Mzinene Fm acts as an aquiclude, likely as a result of the clays within the marine siltstone.

The near-surface geology (0 – 100 m a.s.l) towards the southern end of the iSimangaliso Wetland Park closer to the study area, dips at a shallow angle toward the coastline (Taylor *et al.*, 2006). Due to the lack of access to borehole core data and visible outcrop within the study area itself, the geology

north of the study area has been extracted from Botha *et al.* (2013) and Taylor *et al.* (2006) (Figures 5A and 5B) to produce a preliminary geological cross-section (Figure 5C). Changes in geology can be expected further to the south, however, in-depth research is required to correctly ascertain the geology of the study area itself. The Mzinene aquiclude is known to be extensive across the Maputaland coastal plain and forms the base of the near-surface geology followed by the Uloa Fm which consists of calcarenites interlayered with beds of mudstone (Botha *et al*., 2013). Above this lie the Port Durnford, Isipingo and Kosi Bay Fms which consist of estuary-produced clays, sandy dunes weathered by soil formation and calcareously cemented dune sands, respectively (Botha *et al.*, 2013 and Taylor *et al*., 2006). Lower storativities and hydraulic conductivities in the Port Durnford Fm classify it as an aquitard and create a leaky aquifer between the overlying formations and the formations below (Kelbe *et al.*, 2013). The youngest stratigraphic layer is the Sibayi Fm which was formed by a series of parabolic coastal dunes during the Holocene (Botha *et al.*, 2013 and Taylor *et al*., 2006). The area is then capped by a veneer of weathered material and soils which exhibit no outcrop. Although there is a lack of actual geological data for the study area, the available data for the surrounding areas was sufficient to distinguish between the hydrostratigraphic units (HSU's) important for the hydrodynamics within the study area.

Based on the geology of the area, it can be ascertained that there are three important HSU's in the study area, characterised by distinct hydraulic properties. The rocks of the Zululand Group, specifically the Mzinene Fm formed during the Cretaceous are composed of fine-grained marine siltstones and claystones and act as an aquiclude as a result of their low porosity (n) and hydraulic conductivity (k) (Kelbe *et al.*, 2016). In contrast, the units which are above the aquiclude, have higher hydraulic conductivities and porosities albeit heterogeneous throughout the unit. These rocks are composed of sands, clays and silts that were formed by a combination of aerial, sub-areal and marine processes (Kelbe *et al.*, 2016). These units are largely classified as unconfined aquifers, however, due to the presence of the lower hydraulic conductivity associated with the Port Durnford Formation serving as an aquitard and the Cretaceous aquiclude, it may be classified as a perched or leaky aquifer in some areas (Kelbe *et al.*, 2013 and Kelbe *et al.*, 2016).

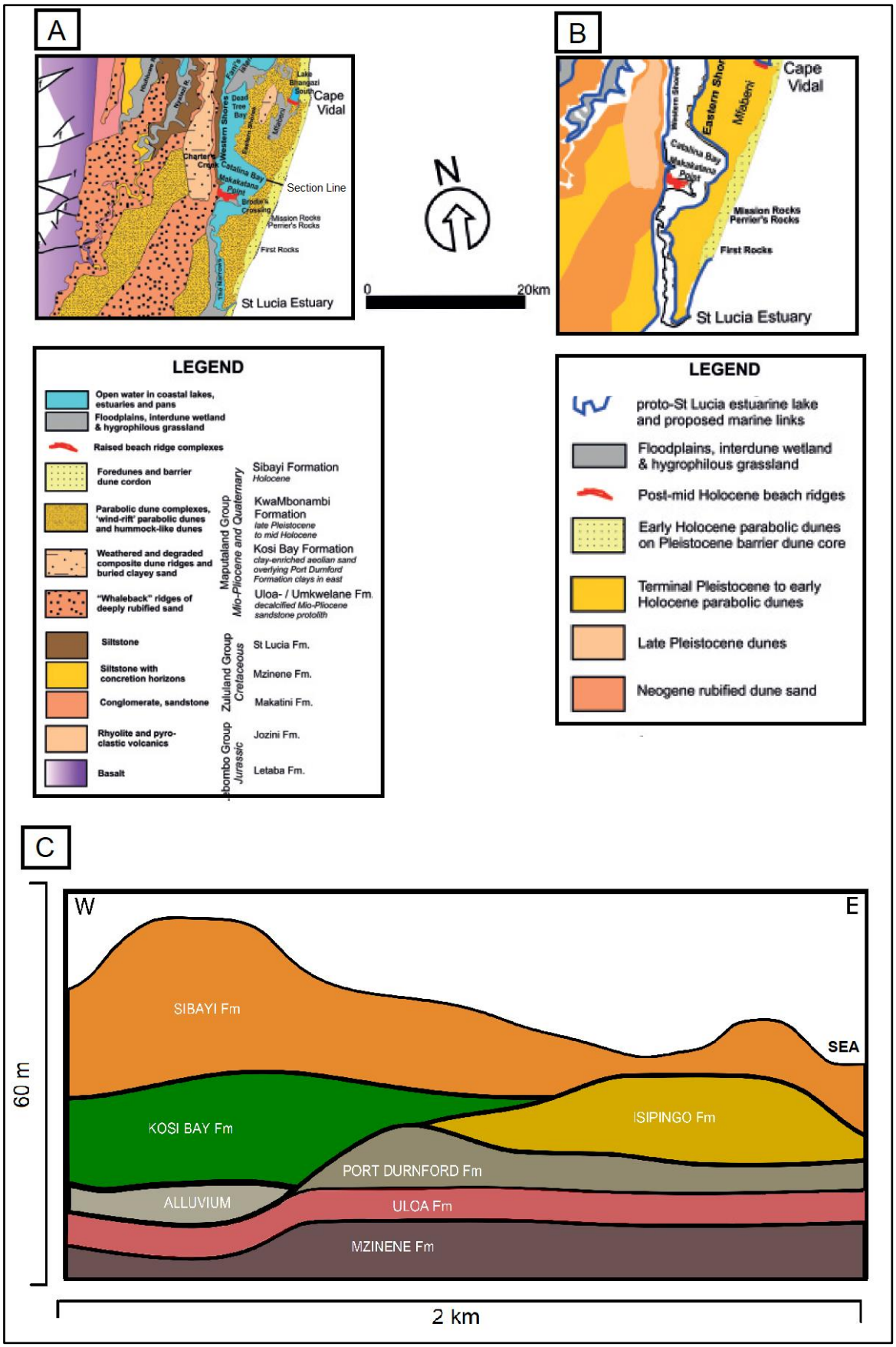

Figure 5 – A) Simplified geological map of the study area and surrounds. B) Surface cover map of the study area and surrounds. C) Simplified geological cross-section of near-surface geology adapted from Taylor et al., 2006 and Botha et al., 2013. Section line indicated in Figure 5A.

3. AIMS AND OBJECTIVES

Various studies with multiple objectives have been conducted on several estuaries and coastal aquifer systems around the world. Due to the dynamic interplay between rainfall, groundwater, the Mfolozi River, wetland, estuary, Lake St. Lucia and the ocean, this particular study area offers a variety of aspects open to research. This research project, however, aims to determine whether mixing occurs between fresh groundwater and seawater by means of both field and laboratory work.
Multiple objectives exist within the scope of this research project. The first utilises both hydrochemical parameters and stable water isotopes to quantify the extent of groundwater mixing, if any, while the second intends to discover and understand the mechanisms which drive or prevent the mixing of waters within the aquifer. The third objective is to gain an overall understanding of water movement and water chemistry within the system through the interplay between various variables in order to better manage water abstraction from the aquifer.

4. RESEARCH DESIGN AND METHODOLOGY

Due to the nature of the research project in the study area, it is imperative to conduct fieldwork as well as lab-based investigations to produce reliable data that may be coupled with historical data regarding water quality parameters from various other sources. One field campaign was conducted for surface mapping and sample collection and to gain a better understanding of the study area.
Laboratory work was conducted both in-house at the University of the Witwatersrand Hydrogeology Laboratory and outsourced to an external laboratory for some analyses.

4.1 – Fieldwork

Google Earth was utilised as an initial mapping tool to understand the spatial layout of the study area and plot potential water sampling points. The boreholes, which are on the properties of residents, businesses and farms were located through the help of residents and using water storage tanks as indicators of wells or boreholes.

To ensure the least effect from human error and chemical reactions during storage and transport, water sampling was conducted using the appropriate measures and techniques. For both surface and groundwater samples, these include:

-taking each sample in duplicate.
-rinsing of water sampling bottles multiple times.
-the filling of water sampling bottles as full as possible to reduce the oxygen available for reaction.

-storing the samples in a cool, shaded area before and during transportation to the laboratories.
-letting the water run through the pipes and/or tap before taking a sample.

For surface water, these include:

-grab sampling from at least 30 cm below the surface.
-ensuring that water does not come into contact with hands or other objects before filling the sampling bottles.
-using a weighted rope to collect samples from the centre of rivers and at least 5 m away from the shoreline.

A Crison MM40 portable multimeter was used to test the pH, electrical conductivity (EC) in μS/cm, total dissolved solids (TDS) in mg/L and temperature in °C of each sample. This was done in the field to acquire an accurate representation of the water in the aquifer. Calibration of the multimeter was performed after every 20 tests using pH 4.01, 7 and 9.21 buffer solutions for pH and a 1413 μS/cm solution for EC calibration. Each sample was labelled using an alpha-numeric code which corresponds to the location and chronological order of sampling as well as a unique field sampling number. The field sampling numbers were used to facilitate sample naming in the field and were written onto each sample bottle using a marker. Plastic bottles with a volume of 1 l were used to sample water for hydrochemical analysis while 20 ml medical grade plastic bottles were used to sample water for stable isotope analysis. Care was taken to keep the samples cool and shaded to prevent UV interference and alteration to the isotopic ratios.

4.1.1 – Samples and Sampling Points

As stated in Section 4.1, the use of Google Earth facilitated the conceptualisation of the study area and samples were subdivided into 6 categories, namely STL for St. Lucia Town, KLV for Khula Village, DKV for Duku Village, EST for estuary, OCN for ocean and UMF for Mfolozi River. These codes were chosen to facilitate the identification of the samples on maps and other figures. All STL, DKV and KLV samples are groundwater samples while the EST, OCN and UMF samples are surface water samples. Sampling point locations can be seen in Figure 1.

The samples were collected between the 25th of January 2021 and the 6th of February 2021. Samples were collected over this time due to the formalities of gaining access to the boreholes as well as getting access to boats for the ocean and estuary. Some inclement weather reduced the time available for sampling due to the possibility of rainwater contaminating samples during collection and analysis while outdoors. The weather during the two weeks period varied with sunshine and clear skies, overcast and humid, cloudy and rain and occasional drizzle and downpours. The general pattern

involved sunny to cloudy mornings on most days followed by afternoon showers and clear evenings. Temperatures were between 17°C and 30°C.

STL Samples – These samples are all groundwater samples and were collected from the St. Lucia town. Boreholes are mostly considered 'wells' by the residents as they are drilled with a hand auger up to 20m deep before which water has already been struck. There are only a few boreholes deeper than 20m in the entire town due to the difficulty associated with deeper drilling as well as the need for a permit to drill using a drilling rig. 12 STL samples (n = 12) were collected and are located within 0.9 and 2 km from the coastline.

KLV Samples – These samples are groundwater samples and were collected from Khula Village which is located on the northern side of the main road (R618) leading to the St. Lucia town. 20 KLV samples (n = 20) were collected between 4.5 and 7.5 km from the coastline.

DKV Samples – These samples are groundwater samples from the Duku Village across the road from Khula Village and on the southern side of the main road (R618). 8 DKV samples (n = 8) were collected between 4 and 6.3 km from the coastline.

EST Samples – These samples are from the estuary which were collected via the dock which extends into the estuary at Sunset Jetty, the estuary boardwalk leading to the beach, as well as from a boat that was used to collect the samples further up the estuary. 6 EST samples were collected (n = 6).

OCN Samples – These samples are seawater samples collected from at least 10 m from the shoreline to approximately 1 km from the shoreline. They were collected by weighted rope and bottle, wading into the water where it was safe and from aboard a fishing boat. 3 OCN samples were collected (n = 3).

UMF Samples – A single sample was collected from the Mfolozi River from a bridge by using a weighted rope and bottle to use as a control for freshwater in the study area.

4.2 – Hydrochemical Analysis

For the analysis of major cations (Mg, Ca, Na, K), anions (Cl, SO_4, HCO_3, CO_3) and any other constituent (Br) which may be considered relevant, Waterlab (Pty) Ltd, an external laboratory approved by SANAS (South African National Accreditation System) was used.

Charge balance error (CBE) calculations were conducted using the formula (Equation 1):

$$CBE = \frac{Sum\ of\ cations - Sum\ of\ anions}{Sum\ of\ cations + Sum\ of\ anions} * 100 \quad (1)$$

The CBE calculation was done to quantify what percentage of the constituents within the water was accounted for in the analyses which were conducted. A high CBE indicates that some constituents are unaccounted for while a low CBE indicates that most constituents are accounted for, although analytical error could also result in a high CBE. The CBE for 70% of the samples is within at least 6%, however, some samples have charge balances of up to 27.7% in KLV-08, 20.0% in sample EST-01 and 10.39% in sample STL-10. The high CBE value for both KLV-08 and STL-10 may be attributed to constituents which may be unaccounted for during the analysis. This could be confirmed by the difference between calculated and measured TDS which may be significantly higher. Sample EST-01 is likely to have a high CBE due to unfiltered particulate matter such as organic matter and nitrates as the sample was taken from the estuary where a multitude of fauna and flora are present which have access to free oxygen. Sample KLV-08 was not utilised for interpretation due to the high CBE.

Due to a potential analytical error for the Br concentration in sample OCN-03, a seawater Br concentration of 67 mg/L adapted from Heeb *et al.* (2014) was used for further analysis and interpretation. AquaChem was used to produce the Piper (1944) and Stiff diagrams to aid with interpretation while XLSTAT (2021) was used to conduct the agglomerative hierarchical clustering analysis (HCA). The HCA was chosen to serve as a means of confirming the results shown by the Piper (1944) plot as it has succeeded in distinguishing between samples of different provenances (Ashley and Lloyd, 1978).

4.3 – Environmental Isotope Analysis

The use of isotopes may serve as a powerful tool in a number of scientific fields. Environmental isotopes in hydrogeology, both stable and radioactive, can be used to determine residence times of groundwater (Torgersen *et al*., 1979), shared water sources, surface and groundwater interaction, directions, and velocities of groundwater flow, as well as characteristics of an aquifer (Kendall and McDonnell, 1998).

To gain an understanding of any isotopic dataset, it must be recorded relative to a standard which is Standard Mean Ocean Water (SMOW) (Craig, 1961). According to Craig (1961), the relative enrichment or depletion of each sample is expressed as $\delta^{18}O$ and $\delta^{2}H$ in permil (‰) and is calculated as follows using Equation 2, for ^{18}O and similarly for ^{2}H:

$$\delta^{18}\mathrm{O}\ (‰) = \left[\frac{\left(\frac{O^{18}}{O^{16}}\right)_{sample}}{\left(\frac{O^{18}}{O^{16}}\right)_{standard}} - 1\right] * 1000 \qquad (2)$$

The Hydrogeology Laboratory at the University of the Witwatersrand was used to analyse the stable isotopes of both $\delta^{18}O$ and $\delta^{2}H$. This was accomplished using the Liquid Water Isotope Analyser – Model 45 – EP (IWA-45EP), which in order to conduct accurate measurements, utilises a high-resolution liquid water isotope analyser. This method has a wide range and is accurate for both highly enriched, highly depleted, and intermediate isotopic ratios and consists of several internal components including a computer, laser analysis system, small-membrane vacuum pump, liquid autosampler, and a system for the reduction of moisture which passes air from the intake through a Drierite® column.

For each of the 52 samples, a handheld pipette was used to deliver a 1 ml aliquot of sample from the 20 ml sample bottle into a 2 ml auto-sampling vial made of glass which was then sealed with a Polytetrafluoroethylene (PTFE) septum lid. Care was taken to add vials of deionised water both before and after analysis of the ocean water samples to prevent potential damage to the equipment. 0.75 µL of sample water was then injected through the PTFE septum of the vial lid into the auto-sampler using a Hamilton microliter syringe, which was subsequently heated to 46°C in order to induce immediate vaporization of the sample under vacuum conditions. The sample which has now been vaporized is transported for analysis into a mirrored chamber which was pre-evacuated. For liquid water samples with a concentration of dissolved salts of up to a minimum of 1000 mg/L, the high accuracy of the laser machine produces results with a precision of 0.2‰ and 1‰ for $\delta^{18}O$ and $\delta^{2}H$, respectively. However, to ensure reliability and maintain consistency in the results, 5 standards were utilised for automatic calibration by the machine between a set number of sample analyses. The standards that were used are shown in Table 1.

Table 1 - Standards used for the calibration of $\delta^{18}O$ and $\delta^{2}H$.

STANDARD	**$\delta^{2}H$**	**$\delta^{18}O$**
5C	-9.2 ± 0.5‰	-2.69 ± 0.15‰
4C	-51.6 ± 0.5‰	-7.94 ± 0.15 ‰
3C	-97.3 ± 0.5‰	-13.39 ± 0.15‰
2C	-123.7 ± 0.5‰	-16.24 ± 0.15 ‰
1C	-154 ± 0.5‰	-19.49 ± 0.15‰

5. RESULTS AND DISCUSSION

Mixing between groundwater in shallow coastal aquifers and seawater is not uncommon. One objective of this study, as previously stated in Section 3, is to gain a localised understanding of mixing and quantify its extent. This section presents and analyses the results of both hydrochemistry as well as stable isotopes to test the occurrence of mixing within the aquifer, as well as attempt to conceptualize the movement of water within the aquifer using a seawater interface model. For the purpose of facilitating data representation and interpretation, several subsections constitute this section and employs graphs, tables, and plots in order to make evident the data collected in this study and their interpretations.

5.1 – Physicochemical Parameters

The physicochemical data for all the samples collected have been tabulated in Appendix A.

pH ranges from 5.18 in sample DKV-07 to 8.05 in sample KLV-14. An arithmetic average of pH for all the samples cannot be given as they are from different sources, hence the average groundwater pH is calculated as 6.52 using 41 samples (n = 41). The higher pH values may be related to either seawater mixing or may possibly originate from a carbonate aquifer within the region such as the Uloa Fm calcarenites.

The EC ranges from as low as 178.7 μS/cm in a Duku Village groundwater sample (DKV-04) to as much as 60500 μS/cm in seawater (Figure 9). The arithmetic average for the EC of groundwater is 606.75 μS/cm. However, this average is skewed by an outlier at the Ski-Club borehole which has an EC of 9260 μS/cm and can be considered brackish. Hence, the average excluding the outlier is 390.42 μS/cm. Figure 9 in Section 5.4.1 shows the EC values of all the collected and measured samples.

The TDS was automatically estimated by the multimeter in the field and displays TDS values in mg/L. The TDS has a range of 114.4 mg/L – 38700 mg/L, with the lowest being a groundwater sample (DKV-04) and the highest being an ocean water sample. The average TDS value for groundwater is 249.86 mg/L excluding the brackish Ski-Club outlier sample (STL-06) which has a TDS of 5930 mg/L. The brackish water at the ski club is likely a result of both mixing with seawater and inland evaporation due to the close proximity to both the coastline and the evaporative pans along the dunes.

The average groundwater temperature is 25.99 °C, with the average surface water temperature being 25.52 °C. The average surface water temperature, however, may not be representative due to varying

climatic conditions, seasons, and slight differences in sampling depths between the ocean, estuary, and river.

The average groundwater level in the study area is approximately 12 m below the surface. This value was obtained from borehole owners who have had their borehole water levels checked in the recent past. Due to the general lack of groundwater level monitoring in the study area itself, the closest monitoring borehole to the study area at Hippo Well (28°19'3.79"S; 32°25'39.40"E), 2 km northeast of sample EST-06, was used to confirm this value and shows an average of 11.57 m (SAEON, 2021). The altitude at this point is 12 m, which results in a water table at approximately 0.5 m above sea level. Figure 6 shows the water level for a period of 15 months. The peaks observed in Figure 6 may be due to periods of rainfall and the troughs due to no rainfall or water abstractions, however, rainfall data for the same time period is unavailable to confirm this.

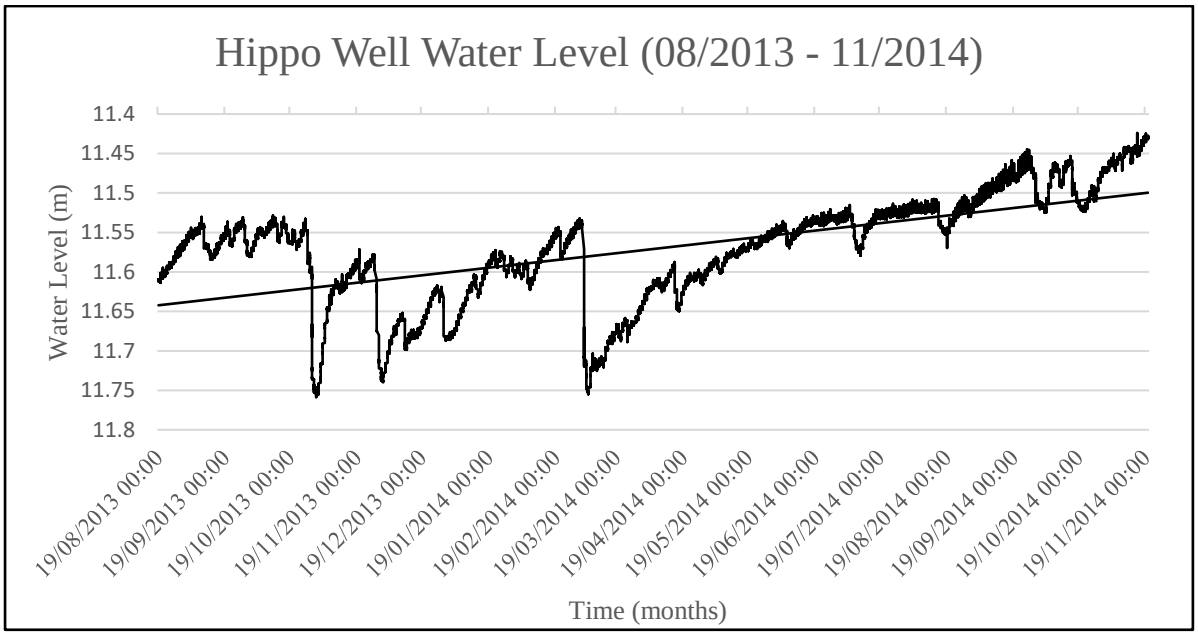

Figure 6 – The barometrically corrected water level at Hippo Well for 15 months. Data courtesy of SAEON (2021).

5.2 – Hydrochemistry

A total of 10 samples were selected for hydrochemical analysis whose results are shown in Table 2. Samples were selected based on their spatial distribution to include a larger sample area as well as samples with variations in TDS and EC values. The Schoeller plot in Figure 7 shows the concentrations in mg/L of major cations (Mg, Ca, Na, K) and anions (Cl, SO_4, HCO_3, CO_3) for the selected samples. It clearly shows a distinction between the concentrations of constituents between the ocean sample (OCN-03) and groundwater samples, with the ocean sample exhibiting higher concentrations of ions, along with STL-06 which may a result of seawater. Figure 7 clearly shows that

Cl, Na, Mg and Ca are the dominant ions in most of the samples indicating enrichment from sources such as seawater and even possibly Ca-rich aquifers, although borehole logs are required to confirm this. Figure 8 shows Stiff diagrams for each sample along with the water type that can be used to group samples. According to the water facies, the samples fall into two categories, those with [HCO_3] < [Cl], and those with [HCO_3] > [Cl]. These categories are discussed in detail in Section 5.2.2.

Table 2 - Hydrochemical data for selected samples.

Sample	Code	pH	Total Alkalinity	$CaCO_3$	HCO_3	CO_3	Cl	SO_4	Br	Na	K	Ca	Mg
				mg/L									
1	STL-01	7.04	88	5	107	5	46	2	0.5	52	2.6	10	7
14	KLV-11	5.58	5	5	5	5	60	43	0.3	50	1.8	3	7
22	DKV-02	7.48	132	5	152	5	46	17	0.5	50	2.7	23	16
28	DKV-08	5.81	5	5	5	5	272	3	0.8	118	8.9	11	32
32	KLV-20	7.29	156	5	190	5	50	16	0.1	64	4.1	26	18
35	STL-06	7.39	520	5	634	5	2399	1110	2.8	1517	85	277	230
36	EST-01	6.94	64	5	78	5	38	20	0.4	65	6.2	12	10
43	STL-10	6.6	56	5	68	5	90	29	0.7	66	1.9	13	23
51	OCN-03	7.88	124	5	151	5	20272	2842	67	11293	630	397	1163

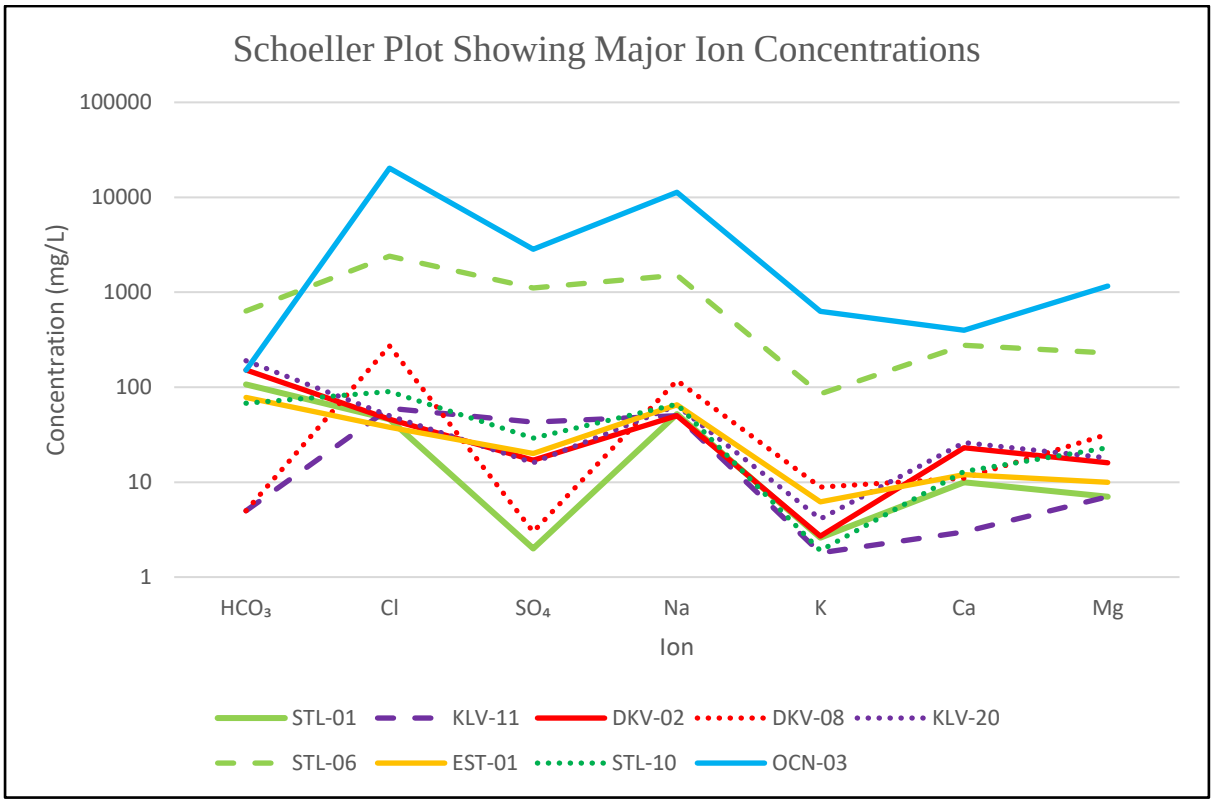

Figure 7 - Schoeller plot showing the concentrations of major anions and cations for selected samples.

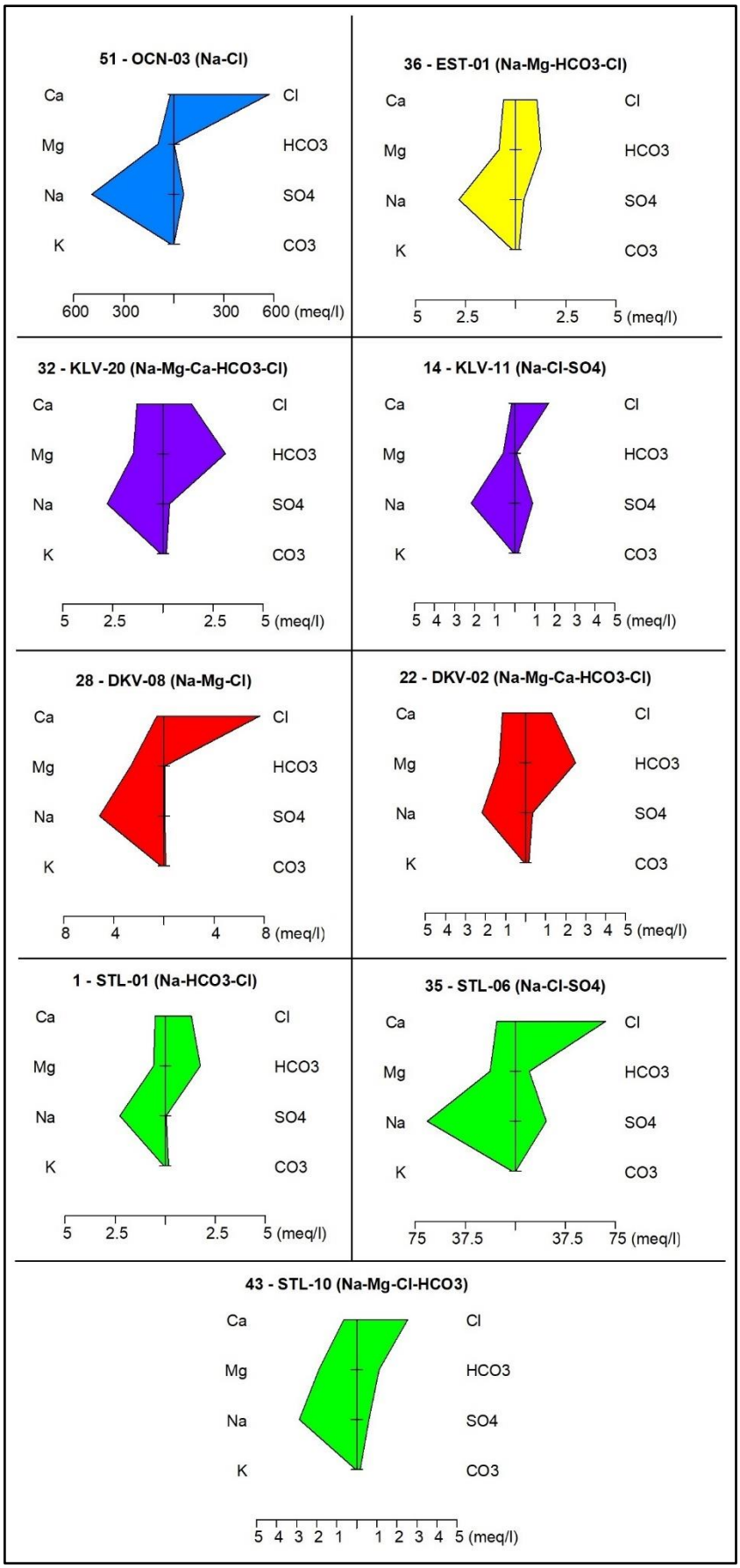

Figure 8 – Stiff diagrams for selected samples showing ion concentrations in meq/L as well as water type.

5.3 – Environmental Isotopes (^{18}O and ^{2}H)

Regression equations developed using Oxygen-18 and Hydrogen-2 data from rainfall produce Meteoric Water Lines (MWL) which can be classified into Global Meteoric Water Lines (GMWL) and Local Meteoric Water Lines (LMWL) (Clark and Fritz, 1997). GMWL's are a combination of LMWL's from various regions over a long time period for which an average has been calculated, while LMWL's are specific to a region that has a particular climate, topographic setting, and other characteristics (Clark and Fritz, 1997). These MWL's are represented in Figures 17 and 18.

The KZN LMWL (KwaZulu-Natal Local Meteoric Water Line) adapted from Van Wyk (2013) is a local meteoric water line developed from 3 years of rainfall data at a station in northern KZN and is defined by:

$$\delta^2\mathrm{H} = 5.6 * \delta^{18}\mathrm{O} + 6.7‰$$

The GMWL used is adapted from (Terzer *et al.*, 2013; GNIP, 2021) using data over a 49-year period and is defined by:

$$\delta^2\mathrm{H} = 7.9 * \delta^{18}\mathrm{O} + 8.72‰$$

A law known as *Fretwell's Law* (Kendall and McDonnell, 1998), serves as a warning to scientists who attempt to utilise isotopes and states that isotopic data should always be coupled with other hydrochemical, geological or hydrological data in order to serve as a means for confirming or rejecting hypotheses tested using other methods (Kendall and McDonnell, 1998). It is for this reason that both the use of stable isotopes and hydrochemistry was employed for the research purposes outlined in Section 3. Table 3 shows a summary of the isotopic values obtained from the samples while Appendices B and C show the raw δ^2H (‰) and $\delta^{18}O$ (‰) data respectively.

Table 3 - Categorized min, max and average $\delta^{18}O$ and δ^2H values.

Water Source	No. of Samples	$\delta^{18}O$ (‰)			δ^2H (‰)		
		Minimum	Maximum	Average	Minimum	Maximum	Average
St. Lucia Boreholes	12	-5.41	-3.88	-4.81	-22.24	-11.05	-16.32
Khula Village Boreholes	20	-5.54	-1.82	-4.55	-21.62	-6.51	-16.42
Duku Village Boreholes	9	-5.77	-2.53	-4.58	-24.27	-10.30	-17.82
Estuary	7	-7.93	-4.94	-6.94	-44.98	-21.05	-36.65
Mfolozi River	1	-7.57	-7.57	-7.57	-41.02	-41.02	-41.02
Ocean	2	-1.35	-1.25	-1.30	-7.12	-3.31	-5.21

5.4 – Seawater Intrusion Detection

5.4.1 - Electrical Conductivity Analysis

Simple maps made using QGIS.org (2021), plots and ionic ratios using hydrochemical data can often provide valuable insight into the hydrogeological and hydrochemical processes occurring and serve as a way of confirming the analysis and results of other methods. EC values provide an initial idea of what can be expected from the data and whether there is significant mixing between seawater and fresh groundwater. A larger sample set of EC data was collected which provides a broader perspective of groundwater quality in the study area. The EC data are represented in Figure 9 and shows relatively low EC values in all the groundwater samples with the exception of STL-06 which was taken nearest to the ocean and close to the estuary bank. The average EC for the groundwater samples is 380.42 µS/cm. According to Carreira (2014), water with EC values below 1000 µS/cm are regarded as freshwater and hence groundwater in the study area may be considered fresh. The absence of samples with very high EC values provides a preliminary indication that seawater intrusion may not be occurring to a great extent within this region.

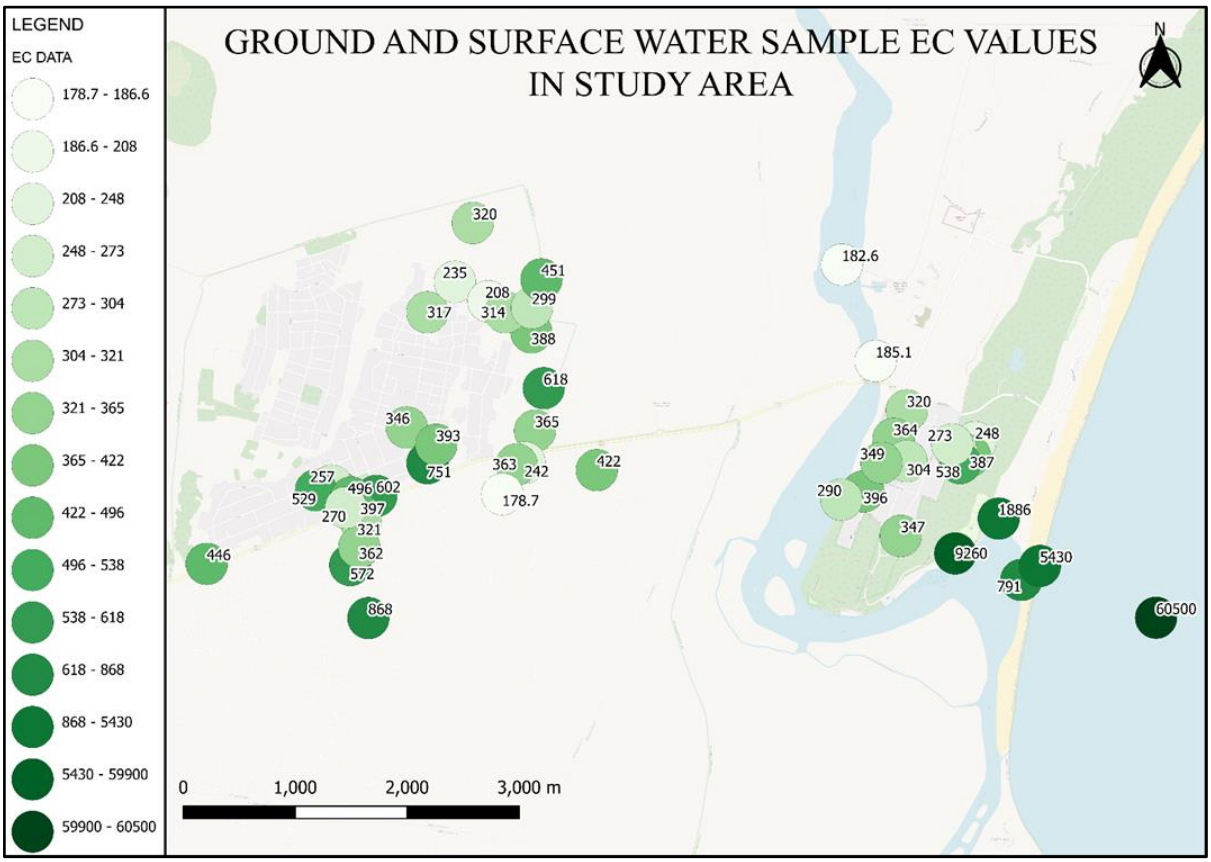

Figure 9 - Map showing ramped EC values for all samples collected with the seawater sample being the highest and groundwater samples below 1000 µS/cm.

5.4.2 – Water Sample Clustering

By grouping the water samples based on hydrochemistry and physicochemical parameters, one may attempt to understand and isolate the various processes occurring within the hydrogeological system. Two methods were used to group the water samples. The Piper (1944) plot (Figure 10) is the first method which shows two distinct water groupings (or clusters), with group 1 represented by yellow-coloured symbols and plotting in the Na-Cl zone and group 2 represented by red-coloured symbols and plotting in the mixing zone between the Na-Cl, Mg-HCO_3 and Na-HCO_3 zones. Figure 10 also shows a shift from HCO_3+CO_3 in group 2 to Cl in group 1 while the group 1 samples are more Ca-rich than the group 2 samples. This indicates that the group 1 samples are dominated by Na and Cl while the group 2 samples are dominated by Ca and HCO_3+CO_3. The Na-Cl type waters (Group 1), with the exception of OCN-03 and STL-06, seen in Figure 10 are likely a result of Cl, Mg and Na recycling. This occurs through precipitation, evaporation, and subsequent infiltration into the subsurface zone in certain areas, as well as some water-rock interaction to produce seemingly mixed waters (Bjørkenes *et al.*, 2006). The Ca-HCO_3+CO_3 waters (group 2) is likely to have gained the additional Ca, HCO_3 and CO_3 from carbonate-rich lithologies. The calcarenites of the Uloa Fm to the west which formed as a result of karst weathering (Kelbe *et al.*, 2013) is considered a water-bearing unit and may be a possible source for the group 2 samples, along with the calcareously cemented dune sands of the Kosi Bay Fm. The actual source of the Ca, however, is still unknown and further research is required. The source for the group 2 samples as well as the depths of the boreholes and residence times may play a role in producing waters, which display distinctly different hydrochemical properties from the group 1 samples.

The satellite image of the study area in Figure 11 shows the location of the samples and the group to which they belong. It is clear that there is no single spatial relationship between the groups which is confirmed by Figure 12 that shows the δ^2H and $\delta^{18}O$ values of the samples. The processes which occur to chemically differentiate these waters likely operate on a scale smaller than the study area itself. Although some samples such as KLV-11 and DKV-08 share similar hydrochemical properties with seawater (OCN-03), they are isotopically different. This confirms that the processes operating to produce the observed hydrochemistry are not controlled by seawater intrusion for those samples. On the other hand, samples DKV-02 and KLV-20 which are part of group 2, exhibit different hydrochemical signatures to that of seawater but are isotopically related. This may be a result of the manner in which groundwater is being abstracted. High abstraction rates from these boreholes may result in the intake of some seawater (Figure 24) and subsequent chemical processes alter the water chemistry, but due to the conservative nature of δ^2H and $\delta^{18}O$, they retain their seawater signatures.

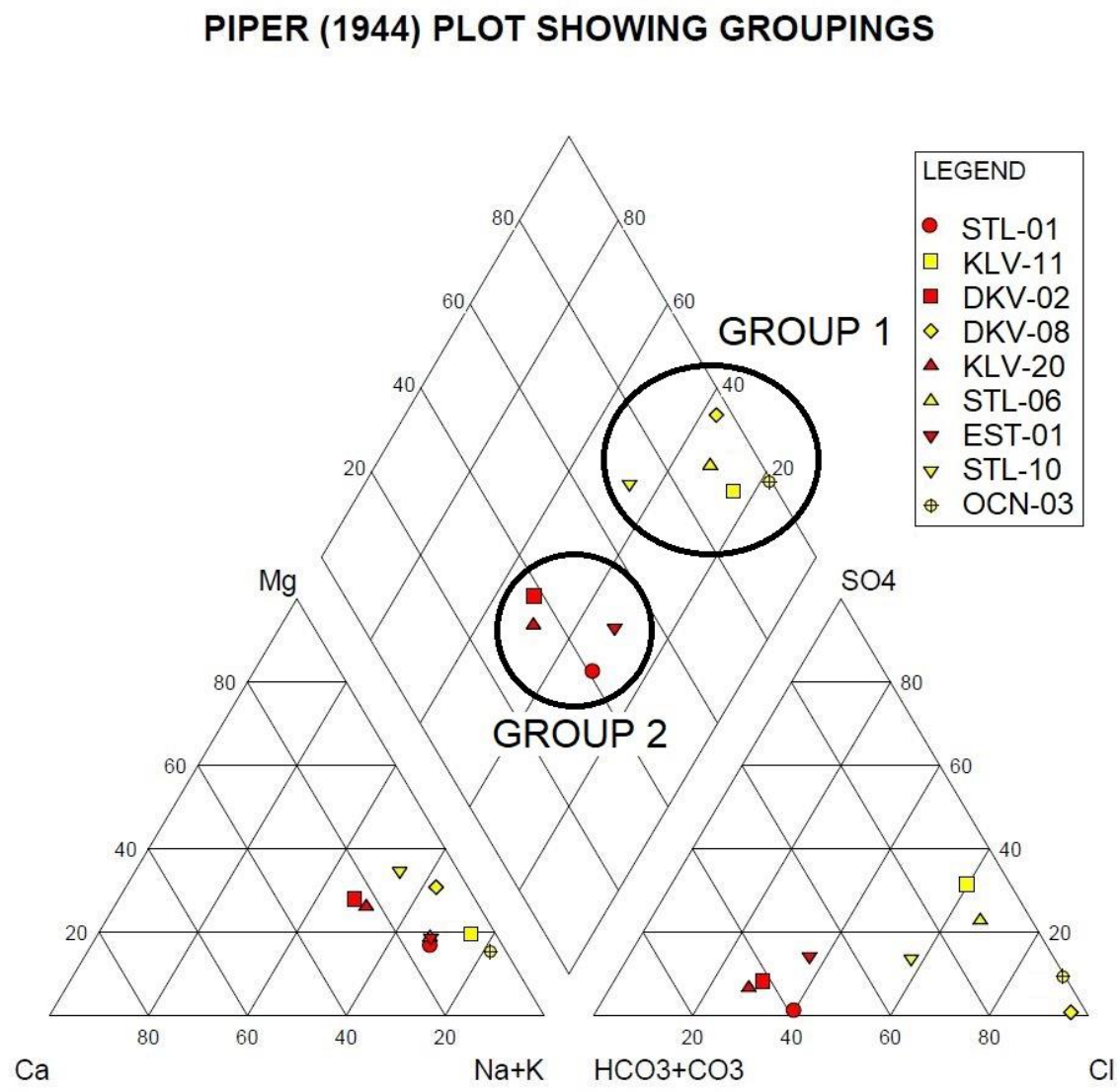

Figure 10 - Piper (1944) plot showing two distinct water groups. Group 1 of Na-Cl type and Group 2 of Ca-HCO_3+CO_3 type.

An agglomerative hierarchical clustering analysis (HCA) was the second method conducted for water sample grouping based on the similarities and uses the weighted pair-group average method to cross the check the groupings seen in the Piper (1944) plot. The HCA was conducted using the same anions and cations as the Piper (1944) plot (Na, K, Ca, Mg, HCO_3, Cl, SO_4) with the addition of Br, stable isotopes δ^2H and $\delta^{18}O$, and physicochemical parameters EC and TDS. The results produced the exact same two groupings (clusters) (Figure 13) as seen in the Piper (1944) plot (Figure 10) where the group 1 samples in yellow are distinctly dissimilar from the group 2 samples in red. This serves to confirm that there are at least two sets of processes operating to produce two distinctly different water groups as seen and discussed.

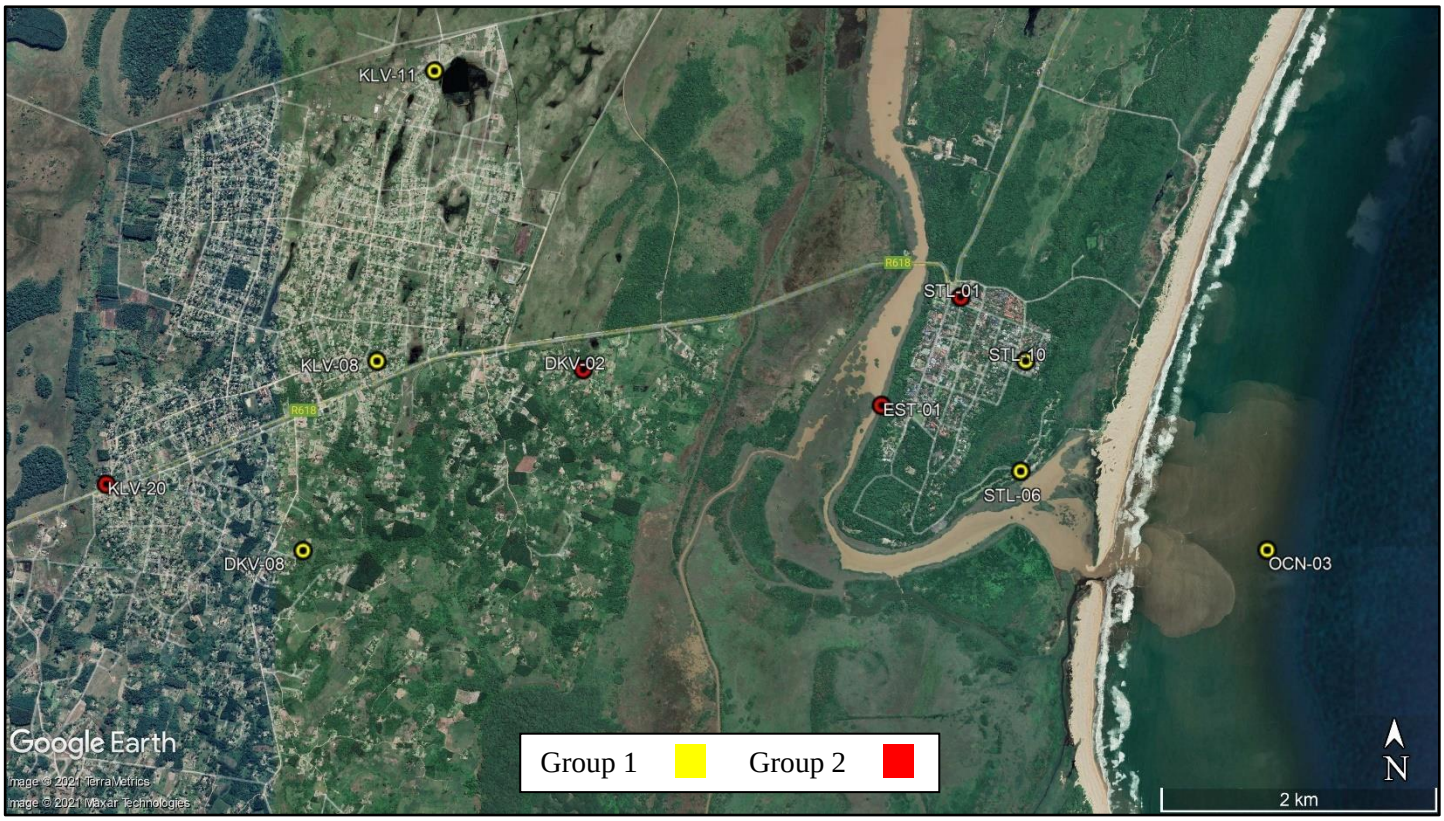

Figure 11 - Satellite image showing the locations of selected sampling points with group 1 samples in yellow and group 2 samples in red (Google Earth, 2021).

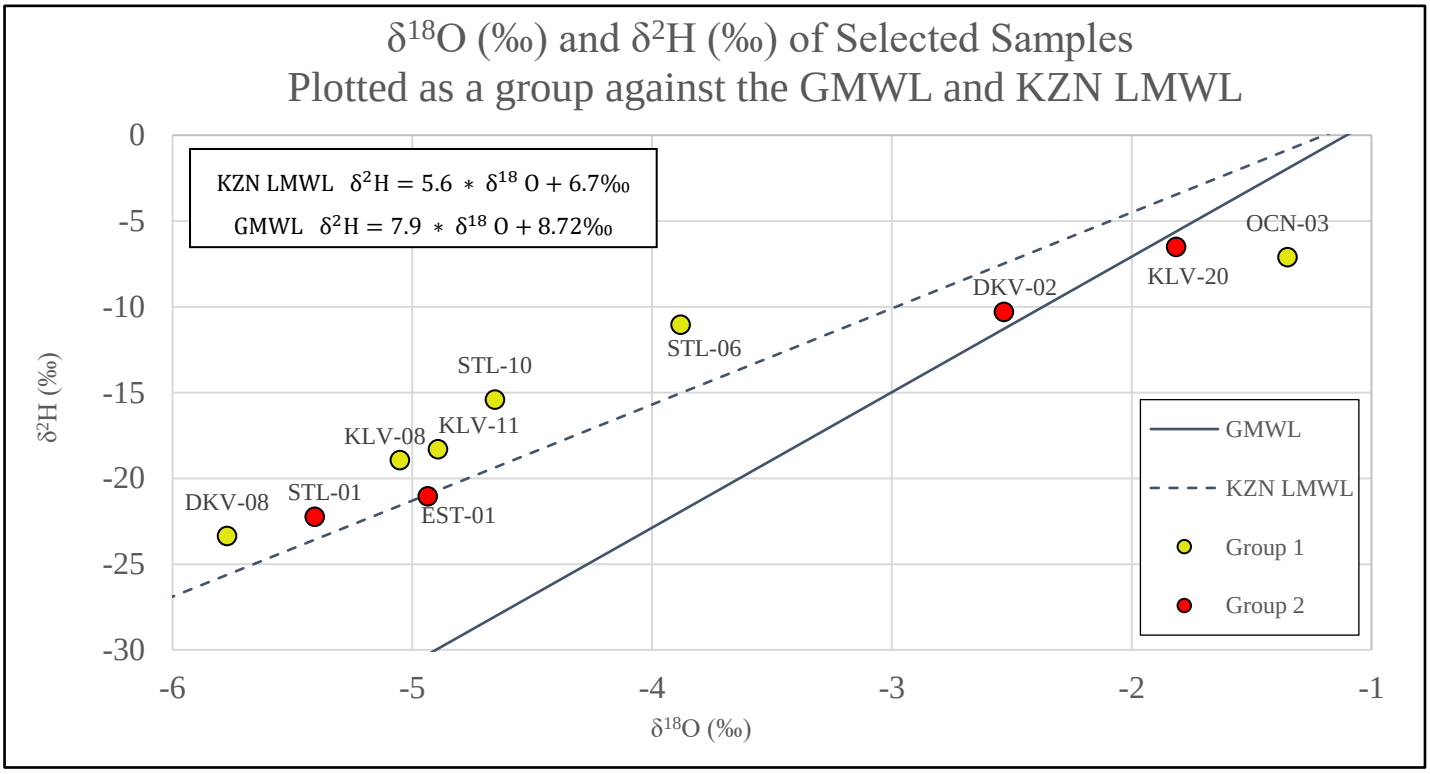

Figure 12 – The δ^2H and $\delta^{18}O$ values of selected samples shown by water group

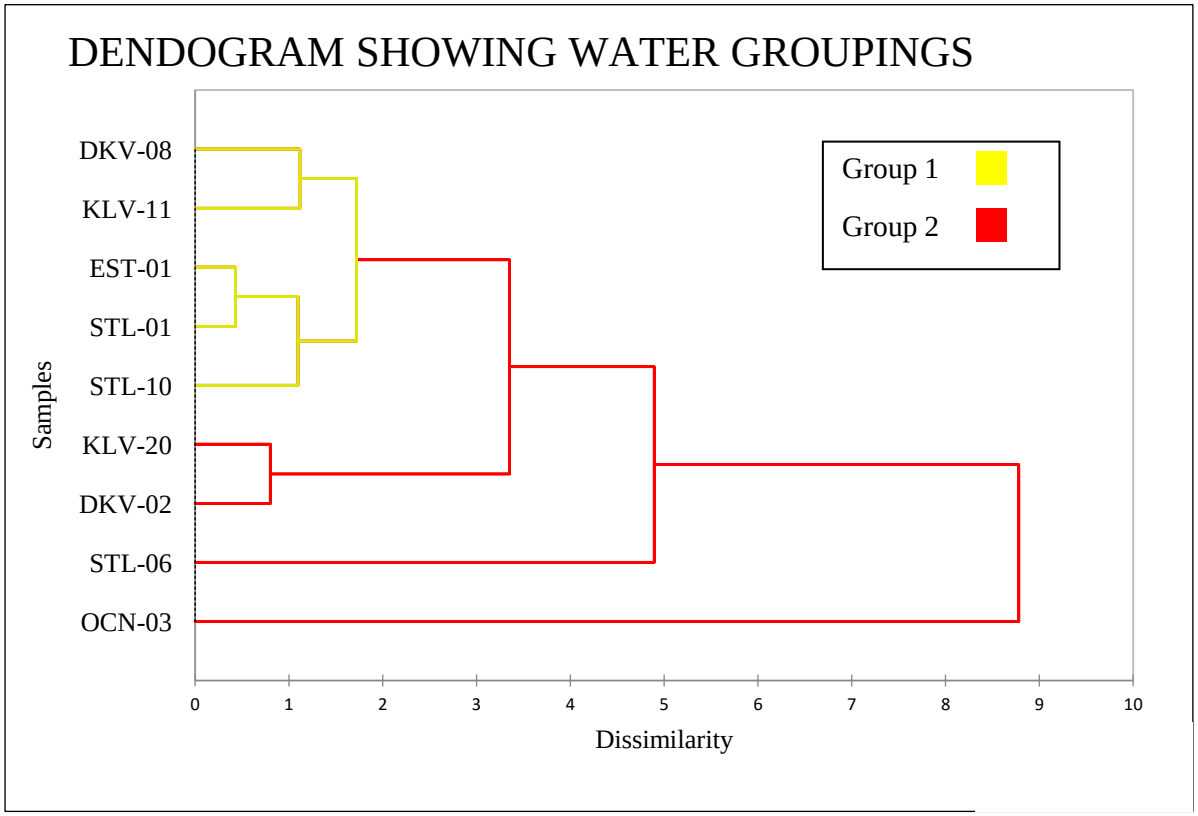

Figure 13 - Dendrogram showing water groups 1 (yellow) and 2 (red) and the dissimilarity between samples and groups due to two sets of processes occurring within the aquifer.

5.4.3 – Ionic Ratio Analyses

By utilising several ionic ratio analyses from various sources, the likelihood of seawater intrusion can be determined. Table 4 shows four ionic ratio analyses each utilising different ions. The Mg/Ca ratio is commonly used as a method for testing whether seawater intrusion is occurring or not in a given dataset. In this case, the Mg/Ca ratios of the samples fall below the seawater ratio indicating that seawater intrusion is not occurring (Maurya *et al.*, 2019). According to Arslan (2013), by plotting the Mg/Ca ratio against Cl and obtaining the R-squared value, the dependency of the Mg/Ca ratio on Cl can be determined. In this case, the R-squared value is 0.03, (Figure 14) representing a low correlation, hence an increase in the Mg/Ca ratio does not have a correlating increase in Cl concentration indicating that the Cl presence in the water is not a result of seawater intrusion.

The Ca/SO_4 ratio is plotted against TDS in Figure 15. Most of the groundwater samples show relatively low Ca/SO_4 ratios with low TDS which indicates that no seawater intrusion is occurring in the area (Lee and Song, 2007). Ca/SO_4 ratios below 1 could indicate cation exchange while Ca/SO_4 ratios above 1 could indicate the dissolution of Ca-minerals (Salem and Osman, 2017). Samples STL-01, KLV-20 and DKV-02 all plot above 1 and are also part of the Group 2 samples (Figure 10).

Should further research prove that the Uloa Fm or Kosi Bay Fm is the source of the Group 2 samples, it would explain the dissolution of Ca minerals within these Fms during periods of residence to produce the group 2 waters of different composition to the group 1 waters (Figure 10).

The Mg/Ca, Na/Cl, SO_4/Cl and Ca/SO_4 ratios are shown in Table 4. These ratios also indicate no seawater intrusion with the green values in Table 4 indicating that the ratio is out of range for seawater mixing with freshwater. The red values in Table 4 are within range for seawater mixing however only 2 out of 9 samples indicate seawater intrusion for SO_4/Cl. Note must be made that these studies were conducted in different geographical areas with different climates and geologies and may not be completely applicable for all seawater intrusion studies.

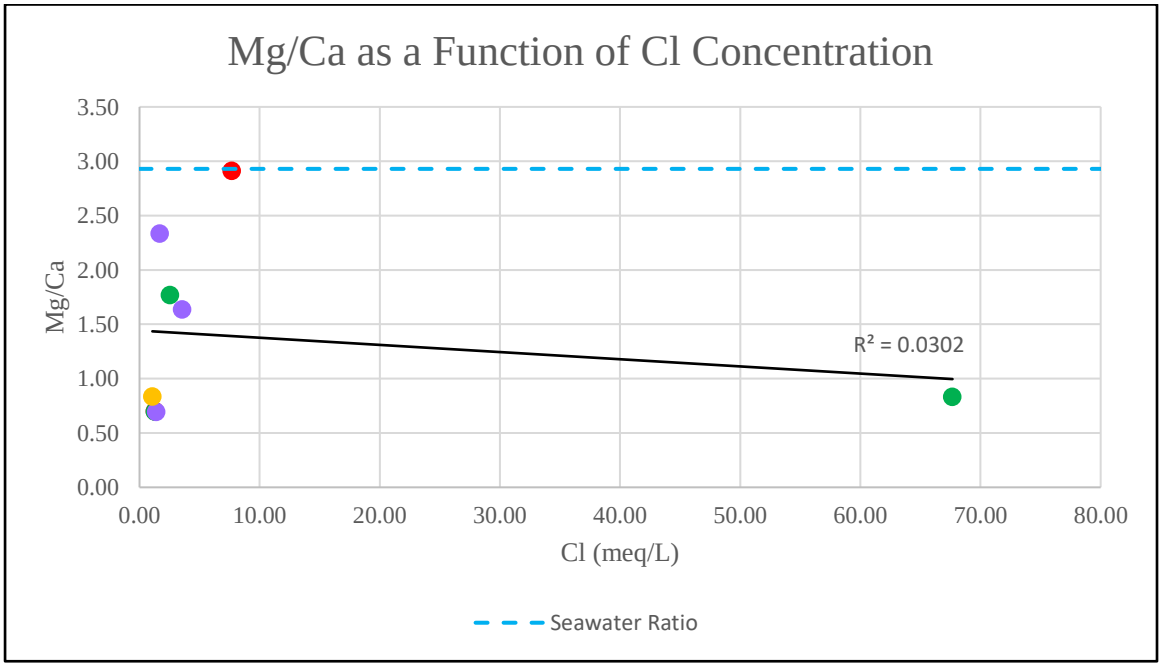

Figure 14 – The Mg/Ca ratios for selected samples plotted against Cl concentration shows low correlation

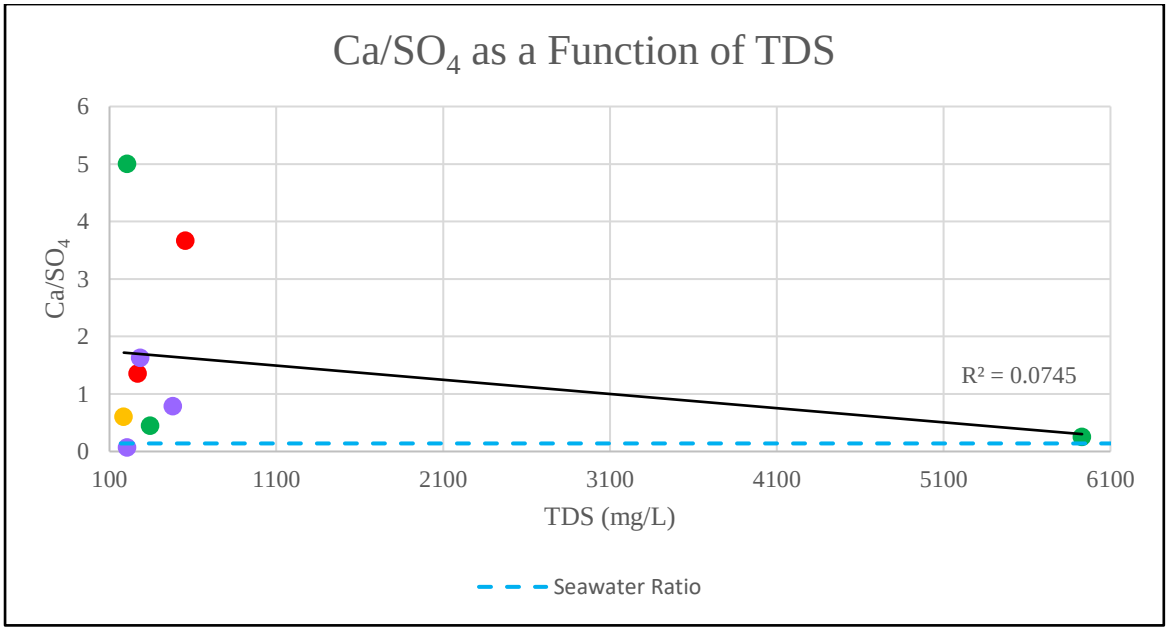

Figure 15 – The Ca/SO₄ ratio plotted against TDS shows low correlation

Table 4 - Multiple ionic ratio analyses indicating a low potential for seawater intrusion.

Ratio	**Mg/Ca**	**Na/Cl**	**SO₄/Cl**	**Ca/SO₄**
Reference	**Maurya *et al.*, 2019**	**Vengosh and Rosenthal, 1994**	**Vengosh *et al.*, 1994**	**Maurya *et al.*, 2019**
Limits	**>5**	**0.86 - 1**	**0.05**	**0.35 - <1**
Sample				
STL-01	0.70	1.13	0.04	0.09
KLV-11	2.33	0.83	0.72	0.06
DKV-02	0.70	1.09	0.37	0.14
DKV-08	2.91	0.43	0.01	1.38
KLV-20	0.69	1.28	0.32	0.13
STL-06	0.83	0.63	0.46	0.16
EST-01	0.83	1.71	0.53	0.12
STL-10	1.77	0.73	0.32	0.13
OCN-03	2.93	0.56	0.14	0.13

5.4.4 – Cl/Br Ratios

The utilisation of a ratio analysis such as the chloride-bromide ratio can serve as a useful tool for understanding the mixing of waters of different sources. In this study area, the Cl/Br ratio was used to gain an understanding of the way that seawater and fresh groundwater mix. The ratio is simply calculated as (Equation 3):

$$Chloride\ Bromide\ Ratio\ = \frac{[Cl]}{[Br]} \quad (3)$$

The graph below (Figure 16) shows a trend that has an ocean sample as well as samples close to the ocean with a high ratio, which then decreases closer to the eastern side of the estuary and increases away from the estuary on the western side. This has been interpreted as the occurrence of a freshwater lens (Figure 24) due to the estuary, as described by Bear *et al.* (1999) which results in the estuarine water suppressing the denser seawater or preventing it from moving laterally through the aquifer. This lens along with the shallow Cretaceous aquiclude likely serve as important buffers for the prevention of seawater intrusion.

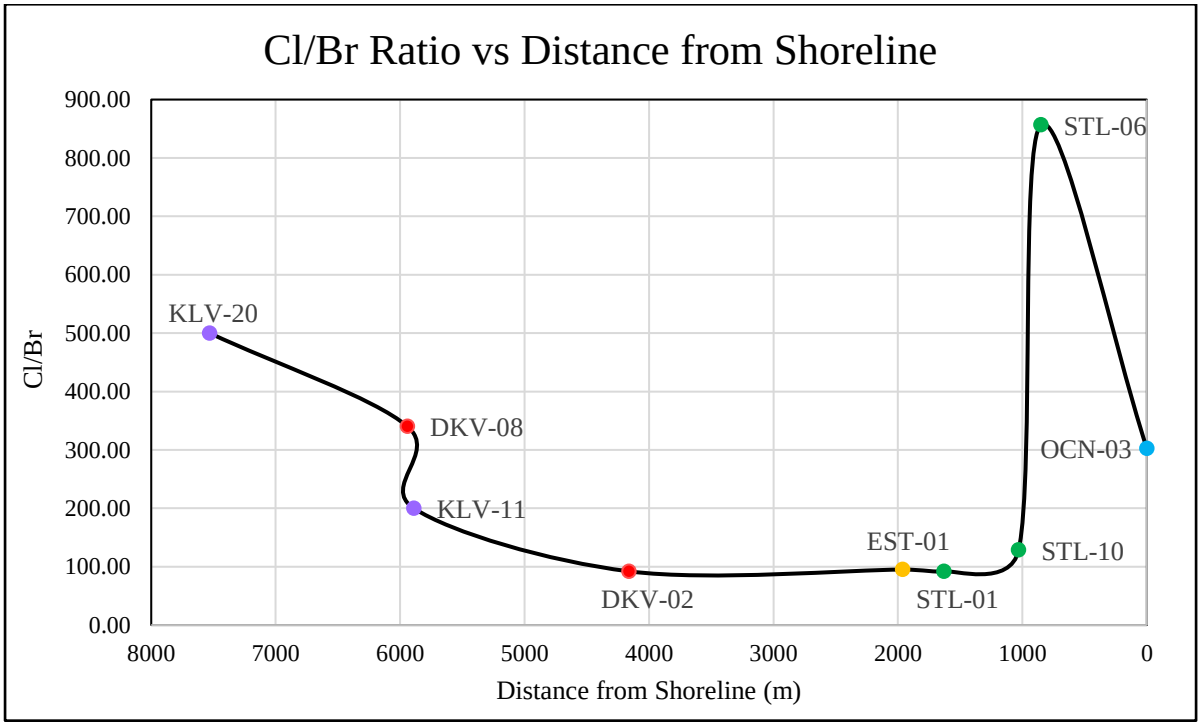

Figure 16 – The Cl/Br ratios for selected samples plotted against distance from the shoreline.

There are samples which have significantly higher Cl/Br ratios compared to seawater. These higher ratios may be attributed to the dissolution and subsequent infiltration of Cl which are present in evaporative pans scattered around the inland and dune regions or as a result of agricultural practices in

the area (Naily, 2018). Sugarcane fields to the west and north-west of the study area may introduce Na and Cl into the root zone of soils by means of continuous irrigation and evapotranspiration as well as through fertilizer and pesticide use, leaving behind salts to be mobilised into the groundwater (Alcalá and Custodio, 2008; Minhas *et al*., 2020). The use of septic tanks in the Khula and Duku villages may also result in high Cl/Br ratios (Alcalá and Custodio, 2008) while precipitation that carries Na and Cl ions from the Southern Ocean may be considered another cause for the high Cl/Br ratios observed in some samples (Taylor, 1991). Animal waste, of which there is no shortage due to the multitude of animals hosted within the iSimangaliso Wetlands Park, is also known to add Cl to groundwater (Srinivasamoorthy *et al.*, 2008). Additionally, Alcalá and Custodio (2008) state that seawater intrusion waters exhibit a Cl/Br ratio between 620 and 680, which is not seen in any of the samples obtained in the study area. These points being made, however, should not disregard the role that seawater mixing may play in the Cl/Br ratios observed. It is likely that some seawater mixing along with a combination of other Na and Cl sources are responsible for the observed trends.

5.4.5 – Environmental Isotope Analysis

The uses for environmental isotopes are outlined in Section 4.3 while this section aims to discuss the results obtained through the analysis of Oxygen-18 and Hydrogen-2 isotopes. Figure 17 is a plot, which shows the $\delta^{2}H$ (‰) vs $\delta^{18}O$ (‰) values obtained from the stable isotope analysis. Paired with the data are the GMWL (Terzer *et al.*, 2013) and the KZN LMWL (Van Wyk, 2013). The slope of the GMWL and LMWL relative to each other indicate that the average relative humidity of the northern KZN is higher than the global humidity during the period when sampling for the LMWL was done (Clark and Fritz, 1997). The GMWL may also not represent the entire earth correctly due to spatial variations in sampling point distributions, which may result in a bias towards areas in the northern hemisphere, which have a higher concentration of sampling points. The data was compared with the KZN LMWL rather than the GMWL as it provides a better average regression of the samples. The data exhibits distinct groupings likely due to different source waters which have undergone various processes resulting in the depletion of the light isotopes during their flow paths. The seawater samples (OCN) plot close to the origin and the SMOW value of 0‰ (Figure 17) as they have not undergone much depletion except due to evaporation from the surface of the ocean. The estuary samples (EST) and the Mfolozi River sample (UMF) are the most depleted waters and plot at the opposite end of the meteoric water lines. A large percentage of the groundwater samples plot in the central region between the seawater and estuary samples, with some outliers showing isotope values closer to that of seawater.

The OCN, EST as well as UMF samples plot below the LMWL as seen in Figure 17 which is expected as they are surface water samples and have undergone some measure of evaporation due to

exposure to the atmosphere. Some groundwater samples exhibit an evaporative signature and plot close to or along the evaporation line (Figure 17). These samples are thought to have undergone evaporation within the pans prior to recharge. The groundwater samples (STL, KLV and DKV) mostly plot either directly on or slightly above the LMWL indicating that there is some direct recharge occurring. This is expected due to high infiltration rates as a result of the geology, topography, and land cover. The KZN LMWL obtained from Van Wyk (2013) was produced from only three years of data (2003 – 2006) and hence may result in recent isotope values deviating from the line and care should be taken not to misinterpret the data obtained.

Understanding the link between the estuary water and groundwater is important for conceptualising the movement of water in the study area. According to Vogel and van Urk (1975), groundwater from a borehole adjacent to a hypersaline section of Lake St. Lucia, north of the study area, has the same $\delta^{18}O$ value as other groundwater samples in the area, indicating that the lateral movement of fresh groundwater prevents the seepage of hypersaline lake water into the alluvial sediments. This process may also be applicable to the areas adjacent to the estuary which as seen in Figure 24, prevents saline ocean water from advancing at shallow depths.

Sample EST-02 is a surface water sample taken from the estuary boardwalk leading to the beach and shows a higher EC (1886 µS/cm), as seen in Figure 9, than that of the other estuary samples due to its proximity to the estuary mouth. The ski club borehole sample (STL-06) has an EC of 9260 µS/cm (Figure 9) and was taken just 570 m away from sample EST-02 and yet has a very different isotopic signature. This may be indicative of minimal surface and groundwater mixing between the estuary and groundwater at this point, and more likely a result of the suppressed seawater which has a higher density and may be pumped from depth at the ski club. Sample STL-06 plots rather close to seawater indicating that mixing has likely occurred in this sample. The average isotopic values of the EST samples are $\delta^{2}H$ (‰) = -36.41 and $\delta^{18}O$ (‰) = -6.91. In Figure 17, 83% of the estuary samples plot away from the groundwater samples, with the exception of EST-01, and hence it can be said that there is a very localised link between the estuary surface water and groundwater which varies along different sections of the estuary.

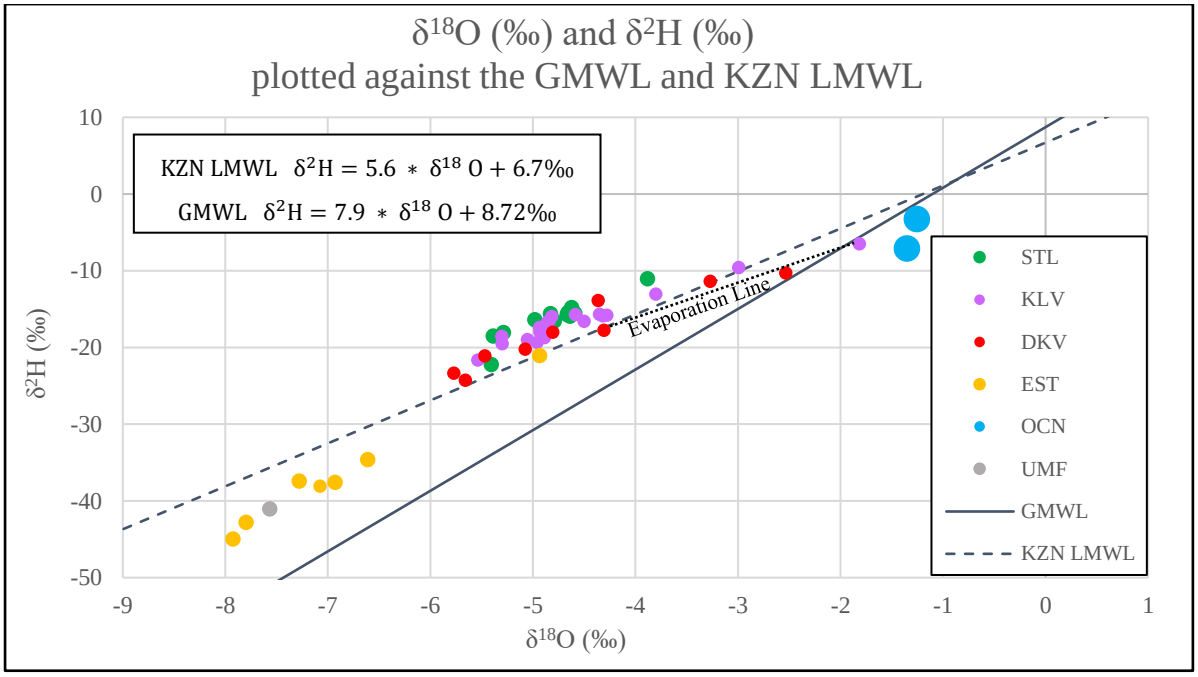

Figure 17 – The $\delta^{18}O$ and $\delta^{2}H$ values plotted against the KZN LMWL and the GMWL.

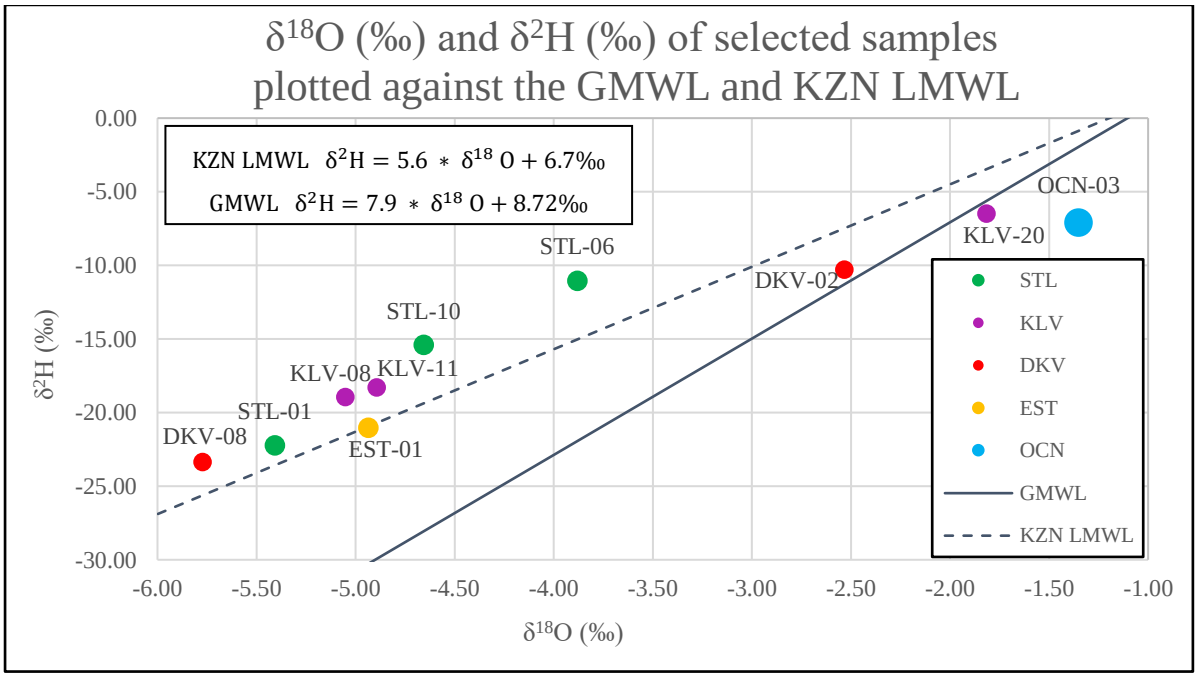

Figure 18 – The colour coded $\delta^{18}O$ and $\delta^{2}H$ values of selected samples plotted against the KZN LMWL and the GMWL.

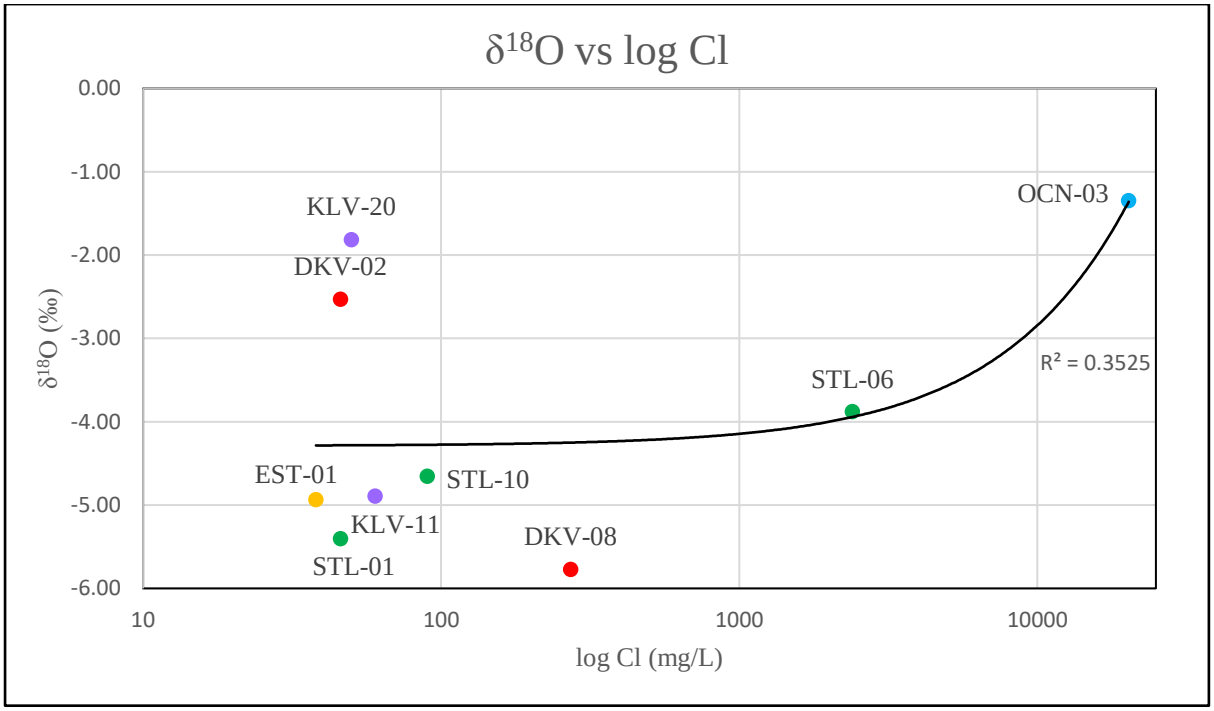

Figure 19 – The $\delta^{18}O$ vs Cl concentration indicating a moderately low correlation.

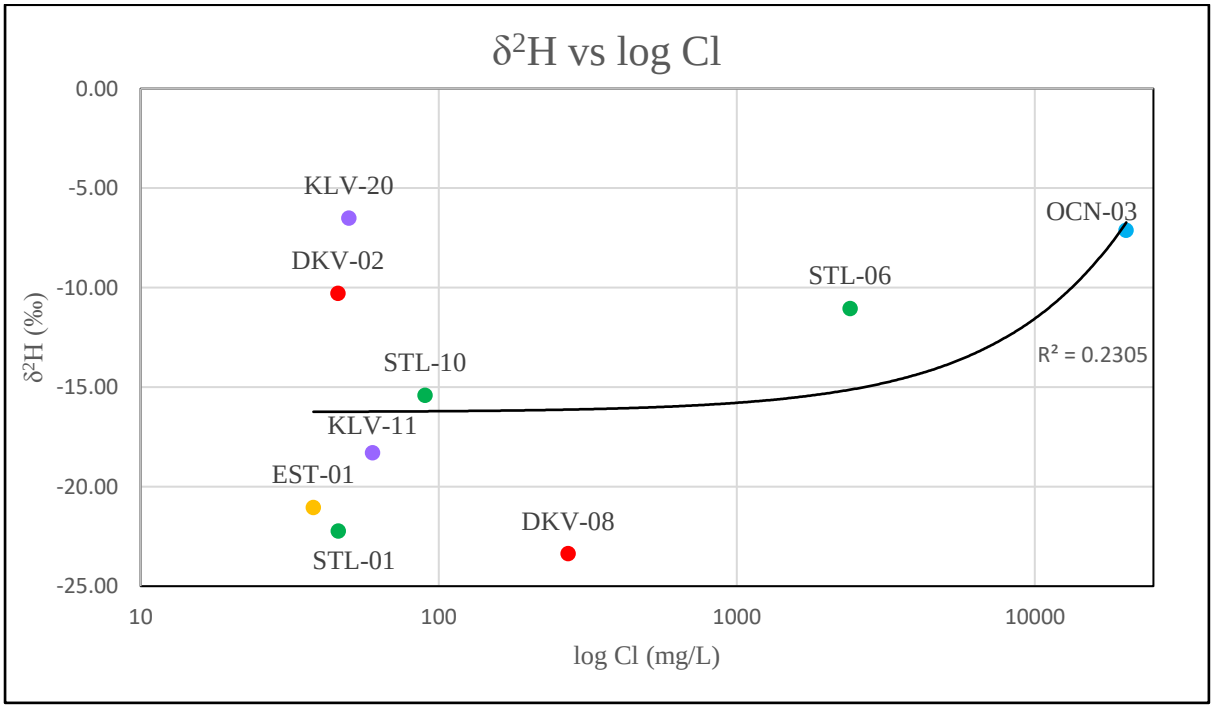

Figure 20 – The $\delta^{2}H$ vs Cl concentration indicating a low correlation.

Although the processes mentioned in Section 5.4.4 may occur to produce the Cl/Br ratios observed, it is likely to affect very localised areas and the Cl may diffuse once its reached the water table. Figure 19, which shows $\delta^{18}O$ values against Cl concentrations also indicates that a mere 35% of the sample's $\delta^{18}O$ values can be attributed to changes in Cl concentration, which also suggests that the Cl has a different source from seawater. Figure 19 also shows two samples (KLV-20 and DKV-02) with lower Cl are enriched in $\delta^{18}O$, while the other samples are progressively depleted in $\delta^{18}O$ while Cl concentration increases. This trend can be expected from waters, which have undergone evaporation to enrich the $\delta^{18}O$ and increase the Cl concentration as seen in the Cl/Br ratio results. The $\delta^{2}H$ values plotted against Cl concentration in Figure 20 exhibit a similar trend to that of $\delta^{18}O$ vs Cl in Figure 19. Samples KLV-20 and DKV-02 have a more enriched $\delta^{2}H$ signature indicating some seawater component. The rest of the samples have progressively depleted $\delta^{2}H$ values indicating recycling as seen with the $\delta^{18}O$ values. Based on the above data and the trends seen, it is unlikely that the high Cl/Br ratios are only a result of Cl from seawater intruding into the aquifer. The possibility of other factors previously mentioned are more likely the cause for most of the samples with the exclusion of STL-06, KLV-20 and DKV-02 which have either similar isotopic values to seawater, a high Cl/Br ratio, or a combination of the two.

5.4.6 – Water Mixing Proportions Using ^{18}O and ^{2}H

Mixing of water above and beneath the surface occurs by means of various processes. The St. Lucia coastline may be considered a tide-dominated coastline due to the presence of the estuary (Masselink *et al.*, 2011). Surface water mixing of freshwater from the Mfolozi River and estuary with seawater at the mouth of the estuary occurs by turbulent mixing, better described as mechanical dispersion which is due to the difference in velocities of the two water bodies (Masselink *et al.*, 2011). Groundwater mixing between seawater and freshwater may be caused by diffusion, advection or mechanical dispersion but is most likely the result of a combination of these processes (Domenico and Schwartz, 1998). Regardless of the manner in which mixing occurs, it is imperative to first quantify the extent of mixing by analysing each sample and calculating its isotopic proportion of seawater to fresh groundwater.

To determine the mixing proportions of each water sample collected, the stable isotope data were again used. This could be done due to the unreactive or conservative nature of the isotopes at relatively low temperatures when in an aquifer, as they will not be enriched or depleted by evaporation or condensation (Gat, 1996). The percentage of seawater in each sample was calculated by using the isotopic ratios of two end members, i.e., ocean water sample OCN-03 and fresh groundwater sample DKV-08 from Duku Village. This ocean water sample was chosen as the end member as it is the sample with the least depleted Oxygen-18 and Hydrogen-2 in the study area. Even

though sample OCN-01 is enriched relative to OCN-03 in both Oxygen-18 and Hydrogen-2, it was not used as it is a reference sample from outside the study area. The freshwater sample chosen was DKV-08 due to it displaying the most contrasting values for both Oxygen-18 and Hydrogen-2 as well as its spatial location. The following equation (Equation 4) adapted from Pulido-Leboeuf (2004) was used:

$$Seawater\ Fraction\ (\lambda) = \frac{\delta^{18}O\ Sample - \delta^{18}O\ River}{\delta^{18}O\ Ocean - \delta^{18}ORiver} \quad (4)$$

To calculate the isotopic ratio of the theoretically mixed samples which lie between the two end members, the following equation (Equation 5) adapted from Salifu *et al.* (2020) was used:

$$\delta^{18}O\ Mix = \delta^{18}O\ Ocean * \lambda + (1 - \lambda) * \delta^{18}O\ River \quad (5)$$

The same method and equations can be employed for δ^2H (‰) and has yielded a similar trend in the fraction of seawater from one end member to the other. When plotting the theoretical mix values, the mixing line is a single linear line represented by a solid black line, which bridges the two end members (Figure 21). Most of the groundwater samples plot above this mixing line which indicates that another level of complexity with respect to source waters is present, i.e., a third end member is present but is not being considered or mixing between the two chosen end members occurs on a small scale which is not sufficient to be a result of large-scale seawater intrusion. Most of the samples plot closer to the freshwater end member indicating that seawater has little effect on the groundwater. Some samples such as KLV-20 and DKV-02, as seen in Figure 18, do plot closer to the seawater end member. This may be a result of the upconing or diffusion of seawater in some areas as it creeps along the base of the aquifer due to suppression by the estuary and blocking by the aquiclude as seen in Figure 24. High rates of groundwater abstraction from these sites may also result in small volumes of seawater being pumped and mixed with the freshwater (Figure 24), which would explain the isotopic values of samples KLV-20 and DKV-02, as well as partially account for their high Cl/Br ratios, in addition to enrichment from evaporation and other sources such as agricultural waste flows and atmospheric Cl. The volume of seawater being incorporated into these boreholes, however, are not large enough to result in high EC values (Figure 9). Figure 22 which shows Na vs Cl concentrations serves to confirm the trend observed in Figure 21 in which groundwater samples plot closer to the freshwater end member, indicating that little to no mixing occurs.

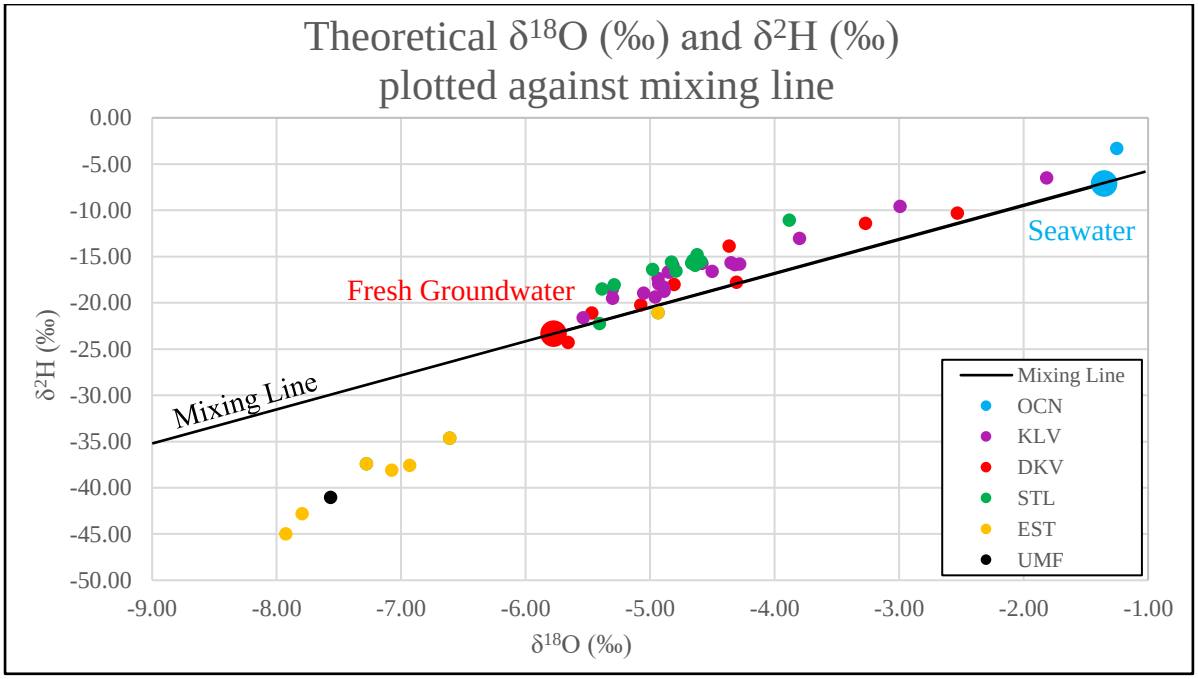

Figure 21 – The theoretical $\delta^{18}O$ and $\delta^{2}H$ values plotted against the mixing line between seawater and fresh groundwater end members.

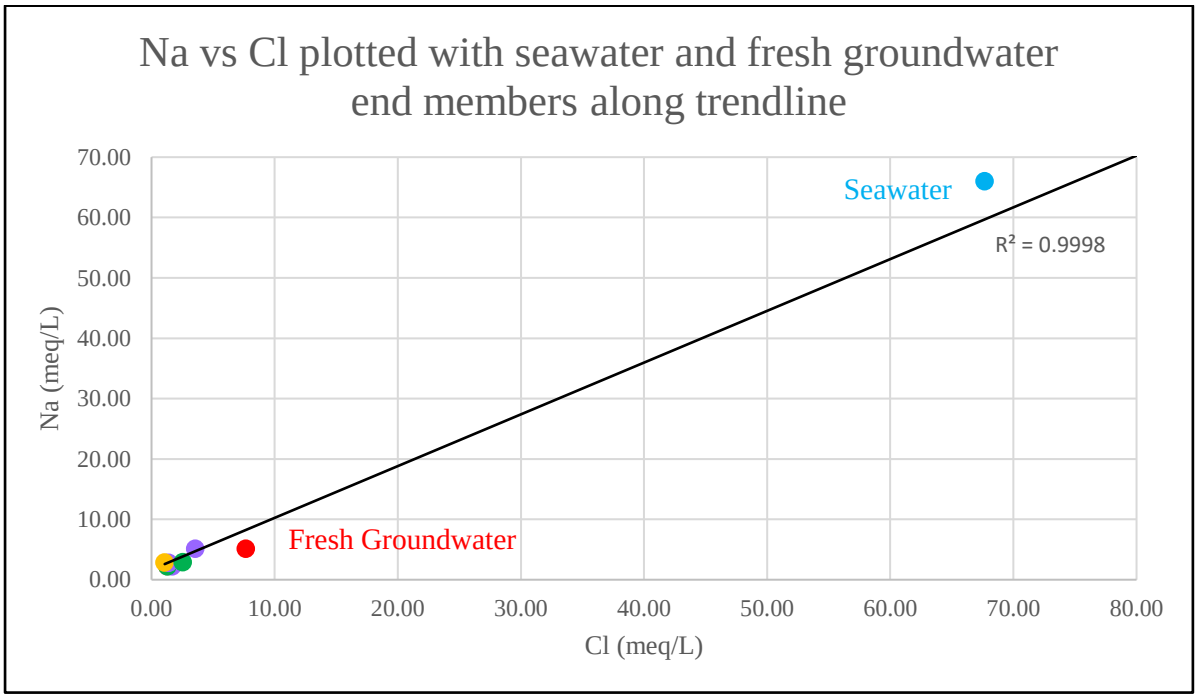

Figure 22 – Concentrations of Na vs Cl in meq/L are plotted along the trendline that shows samples preferentially plot closer to the fresh groundwater end member.

5.5 – Groundwater Hydrodynamics

The movement of water, both above and beneath the surface can be complex to understand, especially when a number of surface water bodies such as rivers, estuaries, wetlands, pans, and lakes play an influential role in and around the study area. Although the aim of this research report was to determine whether mixing between seawater and groundwater occurs, in estuarine systems, this mixing is expected (Acworth, 2019). The interplay between rainfall amount, recharge, changes in sea-level and groundwater abstraction play some role in the hydrodynamics of the St. Lucia area (Acworth, 2019). Seawater intrusion into coastal aquifers is one side of the coin as fresh groundwater has also been known to seep into the ocean through the ocean floor in confined systems (Poeter *et al.*, 2020). As early as the mid-17th century, freshwater from these submarine freshwater springs was pumped from seagoing vessels for onboard utilisation (Poeter *et al.*, 2020). In this case, this scenario is unlikely as the major water-bearing units are unconfined or semi-perched. In order to conceptualise the movement of groundwater, the units above the Cretaceous aquiclude (Mzinene Fm) are considered an unconfined water-bearing HSU, while the Port Durnford Fm is classified as an aquitard.

5.5.1 – Seawater Interface Conceptual Model

The interplay between groundwater at the coastline and seawater produces a seawater wedge, which extends beneath the fresh groundwater due to the contrast in density. The position of this seawater wedge varies from place to place based on groundwater movement, tidal interaction, abstraction, aquifer properties and other factors. The leading edge of this wedge is referred to as the seawater interface, above which lies freshwater and below which lies seawater. The interface can be seen in Figures 23 and 24 and is represented by a zigzag line which in reality grades from saline seawater to brackish water and then to fresh groundwater. The position of this interface can be used to understand how groundwater and seawater behave beneath the surface. Changes in the tide and hydraulic gradient directly affect the position of the seawater interface (Naik, 2018). This model is merely utilised to gain a theoretical understanding and actual data from different depths of boreholes may be used to verify the results seen here.

By using the data obtained in this study as well as data from previous works, a better understanding of the theoretical position of the interface between seawater and fresh groundwater can be determined. This has provided some insight into the objective of how groundwater can be abstracted with minimal risk to the aquifer and the environment as a whole. Based on the depth of the water table and altitude, the theoretical position (depth) of the interface between seawater and fresh groundwater was located.

This can be done using the following equation (Equation 6) adapted from Hiscock and Bense (2014):

$$Zs = \frac{\rho f}{\rho s - \rho f} * Zf \quad (6)$$

where:

- Zs = Seawater interface depth (m)
- ρs = seawater density (kg/m^3)
- ρf = freshwater density ((kg/m^3)
- Zf = altitude of freshwater table (m)

It must be taken into account that this equation may only be used for instances where:

- groundwater within the aquifer flows in a seaward direction.
- the aquifer is homogeneous and unconfined, although an adapted equation may be used for confined aquifers.

The abovementioned criteria are met within the study area. The water-bearing HSU from which water is pumped is considered unconfined. Groundwater is known to flow towards the ocean mostly as a result of the hydraulic gradient along the Maputaland coastal plain, although additional hydraulic head data would be useful to confirm this (Meyer *et al.*, 2001; Mulligan and Charette, 2009). Evidence for groundwater flowing in a seaward direction within the uppermost part of the aquifer is from the $\delta^{18}O$ (‰) and $\delta^{2}H$ (‰) values of sample OCN-02 which has the same source as the estuary samples. A secondary line of evidence for seaward movement of freshwater is the presence of freshwater pans in low relief zones close to the coastline which intersect the water table along the younger sand dunes. Freshwater barbel can be found surviving in these pans which are transported during floods and sustained by the fresh groundwater.

A second equation (Equation 7) is required to compute the density of the water samples based on the TDS. Note must be taken this is merely an estimation and may change based on fluctuations in temperature. For purposes of this study, an average temperature of 26°C was used which was obtained from the groundwater samples taken. The equation was adapted from Collins (1987) and uses TDS and temperature to calculate water density as follows (Equation 7):

$$\rho w = (1 + TDS * 0.695 * 10^{-6}) * 1000 \quad (7)$$

where:

- $\rho w =$ water density (kg/m^3)
- TDS = total dissolved solids (mg/L)

Using the equation (Equation 7) from Collins (1987) and the equation (Equation 6) from Hiscock and Bense (2014), the water level data obtained from private boreholes in the study area, data from Kelbe *et al.* (2016) as well as SAEON monitoring data, and the altitude data from the DEM map (Figure 4), the depth of the seawater interface can be calculated. Due to a lack of groundwater monitoring data close to sampled boreholes, only several water level values were obtained for STL-06 = 9 m, STL-12 = 5 m and KLV-16 = 10 m. These values were obtained from residents in the study area. Figure 23 shows an idealised sketch (not to scale) indicating the theoretical seawater interface beneath the study area based on 3 water level points. The depths of the interface at the 3 points are as follows:

- STL-06 = 44.1 m
- STL-12 = 710.77 m
- KLV-16 = 974.37 m

Based on the changes in depth of the interface with lateral distance, the gradient of the seawater interface appears to be steep. Considering the local geology, it is rather unlikely that the seawater interface extends laterally into the water-bearing HSU (uppermost unconfined or regionally perched aquifer) from which most water is abstracted. This is due to the Cretaceous aquiclude which is approximately 50 m deep, and hence, the seawater interface would be pushed deeper into the units beneath the aquiclude, and seawater would be prevented from intruding on a large scale. However, if high rates of abstraction prevail over a long enough time period, the upconing of seawater as described by Bear *et al.* (1999) and Werner *et al.* (2013) may occur. Seawater may flow along the base of the aquifer and, due to the high volume of abstraction over time, be pumped through the aquifer and Port Durnford aquitard in small quantities as seen in Figure 24. Samples KLV-20 and DKV-02 are suspected to have undergone this process which has resulted in their isotopic signatures being closer to that of seawater than the rest of the groundwater samples, although pumping tests are required to confirm these findings.

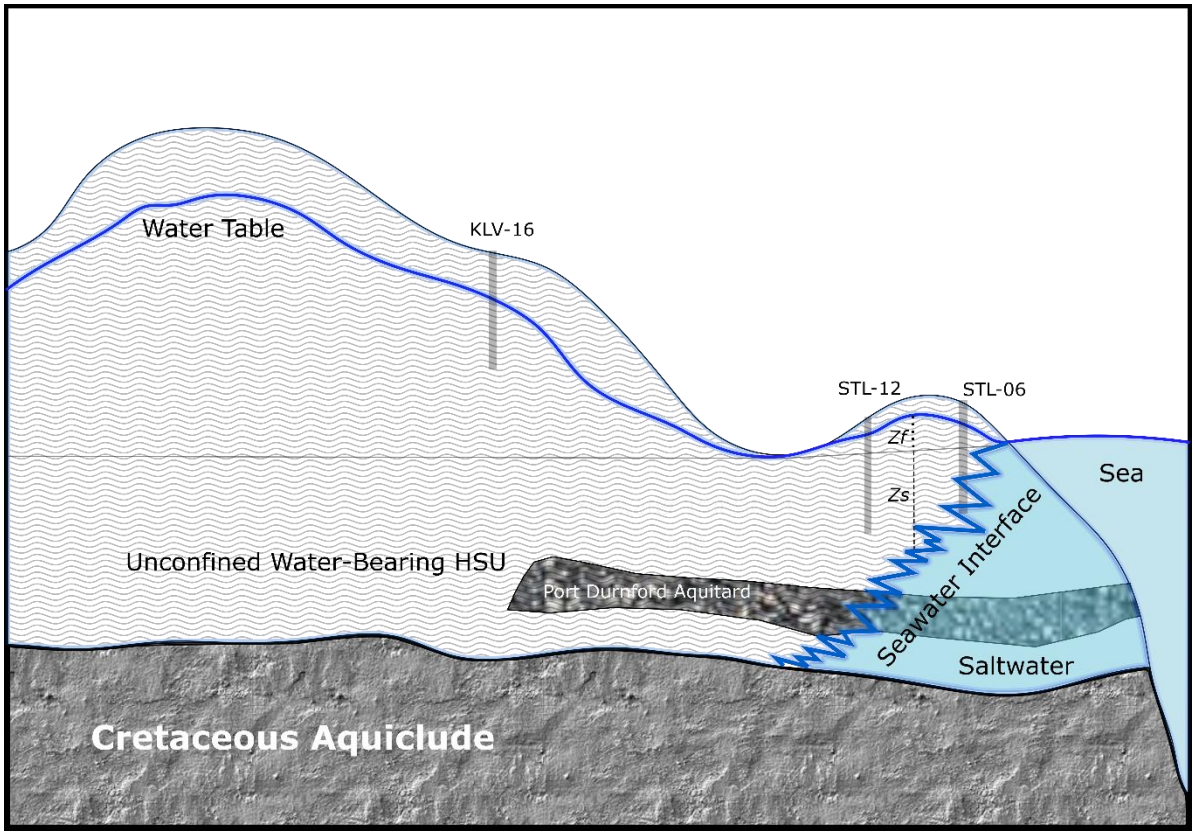

Figure 23 - Model showing the seawater interface at depth within the uppermost aquifer where Zs is the seawater interface depth and Zf is the water table altitude. Adapted and modified from Hiscock and Bense (2014).

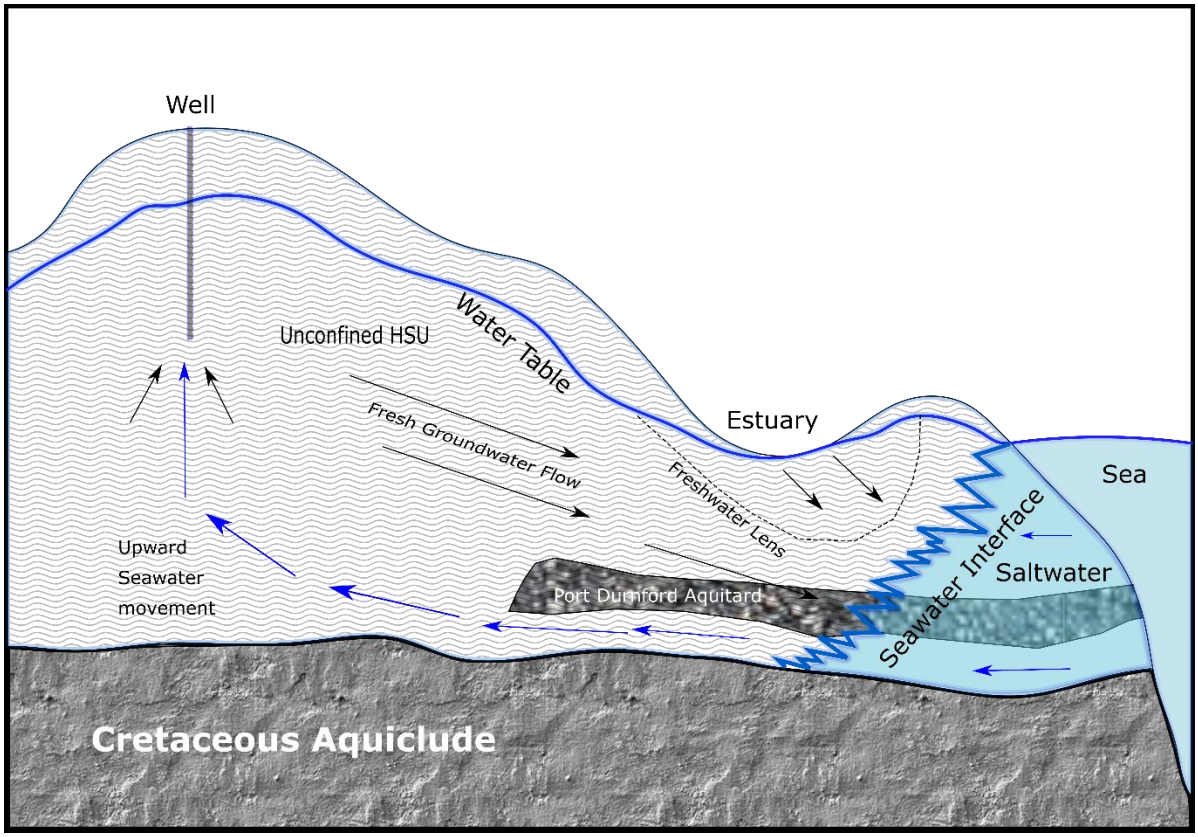

Figure 24 - Model showing the interaction between fresh groundwater and seawater with the unconfined water-bearing HSU, estuary freshwater lens, Cretaceous aquiclude and Port Durnford aquitard.

6. CONCLUSION

The dependency on groundwater coupled with seawater intrusion in St. Lucia and surrounding areas poses a very tangible threat to water security in the area. The hydrodynamics in St. Lucia is rather complex, and should be viewed as a multi-faceted prism, with several factors each playing their role to produce an ever-evolving hydrogeological system. The methods employed in this research report serve to complement each other with respect to the results they have produced. The hydrochemical data clearly shows several sets of processes operating within the system to produce at least two types of waters with differing chemical compositions. Group 1 waters of Na-Cl type are a product of Na, Cl, and minor Mg recycling through evaporation, precipitation, and infiltration. Group 2 waters of Ca-HCO_3+CO_3 type are thought to be a result of water-rock interaction within an aquifer comprised of carbonate lithologies, with the calcarenites of the Uloa Fm and calcareously cemented dune sands of the Kosi Bay Fm both being a possibility, however, further research is required to validate this statement. The increased Ca, HCO_3 and CO_3 concentrations could be the result of long residence times within the aquifer. The Cl/Br ratios among others show that there is little to no mixing between seawater and fresh groundwater. The isotopic data confirm these findings through the theoretical mixing model which shows that there is no mixing in most samples with minor mixing in some samples. In this case, minor mixing refers to samples which plot closer to the seawater end member but do not exhibit the hydrochemistry of seawater. Most of the groundwater samples favour the fresh groundwater end member rather than the seawater end member which could be due to the influence of groundwater flow from the hinterland towards the ocean. The seawater interface model and geology help to conceptualise the HSU's and the movement of groundwater within the aquifer. There appears to be a steep seawater interface which dips below the Cretaceous aquiclude, preventing seawater from intruding into the groundwater in large quantities. This can also be due to the dominance of fresh groundwater that limits saline water incursion in proximity to the ocean. Additionally, the position of the estuary serves to produce a freshwater lens within localised parts of the aquifer which is thought to suppress seawater and prevent shallow lateral mixing on a large scale.

The few samples which exhibit isotopic signatures similar to that of seawater have been interpreted as the lateral flow of seawater along the base of the water-bearing HSU and subsequent upconing due to the possibility of higher groundwater abstraction rates at those points. This represents the onset of seawater intrusion, which is not currently a major concern, however, given the changes associated with climate, rainfall patterns, increased populations, sea-level rise, land use changes, digging of wells and rates of abstraction, this may pose a risk to the quality of groundwater in the St. Lucia area and surrounding villages in the near future. Additionally, increased Cl, Na and Mg concentrations observed in some samples may be attributed to atmospheric sources as well as septic tanks and animal waste from the surrounding wildlife park, as well as agricultural return flows from surrounding

sugarcane farms. Large scale seawater intrusion and agricultural and septic tank waste flows may be combatted by the implementation of water abstraction management through IWRM strategies which will ensure that the groundwater of St. Lucia and its surroundings remains usable for domestic and other purposes in the future. Although tourism and recreation were boosted by the artificial reopening of the estuary mouth, the hydrogeological implications are yet to be seen.

7. RESEARCH LIMITATIONS AND RECOMMENDATIONS

As with any study, it is good practice to acknowledge the limitations and provide recommendations to improve the quality of further research. There are several limiting factors that may have hindered the quality or quantity of work done. In this particular study, the major constraints were financial and temporal, resulting in a limited timeframe to collect and analyse samples, as well as limited funding for field and laboratory work. Additionally, the research conducted here was done so at the onset of the artificial reopening of the estuary mouth in January 2021. This may have produced results which are biased towards that particular point in time and may not be a true representation of the system after some months or years have passed. Due to the financial and time constraints mentioned, a second sample set during the dry season (April - September) could not be taken and hence due to the dilution effect, some hydrochemical concentrations, water levels and other aspects may be different to what was seen during field work in the wet season. This may be especially true due to the combined 655.57 mm of rainfall received in Jan and Feb of 2021 alone, which comprises over 50% of the mean annual rainfall.

Recommendations for further research include detailed geological mapping through borehole core analysis and geophysical methods, quantifying water residence times using tritium isotope analysis as well as continuous hydrochemical and groundwater level monitoring within areas considered at higher risk to seawater intrusion. Sampling water from boreholes which tap the Uloa and Kosi Bay Fms may be of use to determine if these aquifers are the source for the Group 2 waters. Analysis of larger sample sets may also improve confidence in the results obtained from this study. Continuous analysis of stable isotopes in precipitation and groundwater may also aid in understanding groundwater movement including recharge areas and mixing. The analysis of nitrates, nitrites and nitrogen isotopes may also prove useful in tracing pollution sources within the area. In-depth hydrochemical analyses may also allude to any water-rock interaction which may be occurring, and which may explain some of the trends observed. Gaining access to additional historical rainfall and groundwater level data may help understand the relationship between rainfall and groundwater level. This will show whether the water table is being raised by increased rainfall and groundwater flow or seawater flow or whether it is being lowered by a lack of rainfall or water abstractions. Monitoring the rate of water abstractions

together with water balance calculations may also prove useful for understanding the limits to which water can be pumped safely without the risk of seawater upconing. It cannot be said with certainty that the groundwater in the town of St. Lucia and Khula and Duku Villages are safe for consumption due to a lack of bacteria analyses and extensive hydrochemical data which is also highly recommended.

8. REFERENCES

Acworth, I., (2019). Investigating groundwater. CRC Press, London, p 598

Adams. J, (2021). Current ecological state of the St Lucia Lake & mouth – Symposium Presentation, Available at: https://isimangaliso.com/all-downloads/documents/#

Alcalá, F.J. and Custodio, E., (2008). Using the Cl/Br ratio as a tracer to identify the origin of salinity in aquifers in Spain and Portugal. *Journal of Hydrology*, *359*(1-2), pp.189-207.

Arslan, H., (2013). Application of multivariate statistical techniques in the assessment of groundwater quality in seawater intrusion area in Bafra Plain, Turkey. *Environmental monitoring and assessment*, *185*(3), pp.2439-2452.

Ashley, R.P. and Lloyd, J.W., (1978). An example of the use of factor analysis and cluster analysis in groundwater chemistry interpretation. *Journal of Hydrology*, *39*(3-4), pp.355-364.

Bate, G.C., Whitfield, A.K. and Forbes, A.T., (2011). A review of studies on the Mfolozi estuary and associated flood plain, with emphasis on information required by management for future reconnection of the river to the St. Lucia system. WRC Report No. KV 255/10. Water Research Commission, Pretoria.

Bear, J., Cheng, A.H.D., Sorek, S., Ouazar, D. and Herrera, I. eds., (1999). Seawater intrusion in coastal aquifers: concepts, methods and practices (Vol. 14). Springer Science & Business Media.

Bjørkenes, M.S., Haldorsen, S., Mulder, J., Kelbe, B. and Ellery, F., (2006). Baseline groundwater quality in the coastal aquifer of St. Lucia, South Africa. In Urban groundwater management and sustainability (pp. 233-240). Springer, Dordrecht.

Botha, G.A., Sylvi Haldorsen,S. and Naomi Porat, N., (2013). Geological history. Ecology and Conservation of Estuarine Ecosystems: Lake St Lucia as a Global Model. Cambridge University Press, Cambridge, pp.48-61.

Brown, J.S., (1925). *A study of coastal groundwater, with special reference to Connecticut* (No. 537). USGS, Govt. Print. Off. Series no. 537. DOI: 10.3133/wsp537

Carreira, P.M., Marques, J.M. and Nunes, D., (2014). Source of groundwater salinity in coastline aquifers based on environmental isotopes (Portugal): natural vs. human interference. A review and reinterpretation. *Applied Geochemistry*, *41*, pp.163-175.

Chrystal, R.A.L., (2013). Anthropogenic impacts and biophysical interactions in Lake St Lucia (Doctoral dissertation).

Clark, I.D. and Fritz, P., (1997). Environmental isotopes in hydrogeology. CRC press.

Cleverly, RW* and Bristow, J., (1979). Revised volcanic stratigraphy of the Lebombo monocline. South African Journal of Geology, 82(2), pp.227-230.

Clulow, A.D., Everson, C.S., Mengistu, M.G., Jarmain, C., Jewitt, G.P.W., Price, J.S. and Grundling, P.L., (2012). Measurement and modelling of evaporation from a coastal wetland in Maputaland, South Africa. *Hydrology and Earth System Sciences*, *16*(9), pp.3233-3247.

Collins, A., G., (1987). Properties of produced waters, in Bradley, H., B., eds., *Petroleum Engineering Handbook*: Dallas, SPE, p. 24-1–24-23.

Connell A.D. and Porter S.N., (2013). The marine environment. Ecology and Conservation of Estuarine Ecosystems: Lake St Lucia as a Global Model. Cambridge University Press, Cambridge, pp.63-76.

Craig, H., (1961). Standard for reporting concentrations of deuterium and oxygen-18 in natural waters. *Science*, *133*(3467), pp.1833-1834.

Domenico, P.A. and Schwartz, F.W., (1998). Physical and chemical hydrogeology (Vol. 506). New York: Wiley.

Falkenmark M. and Widstrand C. (1992). Population and water resources: a delicate balance. *Population Bulletin*, Nov;47(3):1-36. PMID: 12344702.

Gat, J.R., (1996). Oxygen and hydrogen isotopes in the hydrologic cycle. *Annual Review of Earth and Planetary Sciences*, *24*(1), pp.225-262.

GNIP/IAEA, (2021). Global Network of Isotopes in Precipitation/International Atomic Energy Agency: The GNIP Database, available at: https://nucleus.iaea.org/wiser/index.aspx (last access: 09/11/2021).

Google Earth 7.3.4.8248. (2021). St. Lucia and Surrounds, 28°22'46.40"S, 32°23'43.53"E, eye alt 9.07km, MAXAR Technologies and TerraMetrics 2021., viewed 20 Sep 2021. <http://www.google.com/earth/index.html>.

Gordon, N., Perissinotto, R. and Miranda, N.A.F., (2016). Microalgal dynamics in a shallow estuarine lake: Transition from drought to wet conditions. Limnologica, 60, pp.20-30.

Heeb, M.B., Criquet, J., Zimmermann-Steffens, S.G. and Von Gunten, U., (2014). Oxidative treatment of bromide-containing waters: formation of bromine and its reactions with inorganic and organic compounds—a critical review. *Water Research*, *48*, pp.15-42.

Hiscock, K.M. and Bense, V.F., (2014). Hydrogeology: principles and practice, 2nd Edition, John Wiley & Sons.

IWP, (2011). Lake St Lucia: understanding the problem and finding the solution, Background Information Document, Available at: https://isimangaliso.com/all-downloads/documents/

IWP, (2019). iSimangaliso Wetlands Park annual report 2019/2020, Available at: https://isimangaliso.com/all-downloads/reports/

Kelbe, B.E., Grundling, A.T. and Price, J.S., (2016). Modelling water-table depth in a primary aquifer to identify potential wetland hydrogeomorphic settings on the northern Maputaland Coastal Plain, KwaZulu-Natal, South Africa. Hydrogeology Journal, 24(1), pp.249-265.

Kelbe, B.E., Taylor, R.H., Haldorsen, S., Perissinotto, R. and Stretch, D.D., (2013). Groundwater hydrology. Ecology and Conservation of Estuarine Ecosystems: Lake St Lucia as a Global Model. Cambridge University Press, Cambridge, pp.151-167.

Kendall, C. and Caldwell, E.A., (1998). Fundamentals of isotope geochemistry. In *Isotope tracers in catchment hydrology* (pp. 51-86). Elsevier.

Lee, J.Y. and Song, S.H., (2007). Groundwater chemistry and ionic ratios in a western coastal aquifer of Buan, Korea: implication for seawater intrusion. *Geosciences Journal*, *11*(3), pp.259-270.

Loáiciga, H.A., (2003). Climate change and groundwater. Annals of the Association of American Geographers, 93(1), pp.30-41.

Maro, A.Z., (2012). *Modelling hydrological responses to land use and climate change: The Mfolozi Catchment* (MSc dissertation), University of KwaZulu-Natal.

Masselink, G., Hughes, M. and Knight, J., (2011). Introduction to coastal processes and geomorphology 2nd Ed. Great Britain, UK.

Maurya, P., Kumari, R. and Mukherjee, S., (2019). Hydrochemistry in integration with stable isotopes ($\delta^{18}O$ and δD) to assess seawater intrusion in coastal aquifers of Kachchh district, Gujarat, India. *Journal of Geochemical Exploration*, *196*, pp.42-56.

McCarthy, T. and Rubidge, B., (2005). The story of Earth and Life A southern African perspective on a 4.6-billion-year journey. published by Struik. Cape Town, p.333.

Meyer, R., Talma, A.S., Duvenhage, A.W.A., Eglington, B.M., Taljaard, J., Botha, J.P., Verwey, J. and Van der Voort, I., (2001). Geohydrological investigation and evaluation of the Zululand coastal aquifer. Water Research Commission Report, 221(1), p.01.

Minhas, P.S., Ramos, T.B., Ben-Gal, A. and Pereira, L.S., (2020). Coping with salinity in irrigated agriculture: Crop evapotranspiration and water management issues. Agricultural Water Management, 227, p.105832.

Mook, W.G., (2000). Environmental isotopes in the hydrological cycle. Principles and Applications - reprinted with minor corrections, Volume I – Introduction, theory, methods, review.

Morris, T., Lamont, T. and Roberts, M.J., (2013). Effects of deep-sea eddies on the northern KwaZulu-Natal shelf, South Africa. *African Journal of Marine Science*, *35*(3), pp.343-350.

Mulligan, A.E. and Charette, M.A., (2009). Groundwater flow to the coastal ocean. *Elements of Physical Oceanography: A derivative of the Encyclopedia of Ocean Sciences*, *465*.

Naik, P.C., (2018). *Seawater Intrusion in the Coastal Alluvial Aquifers of the Mahanadi Delta*. Springer International Publishing.. 1st ed. 2018 edition. P121

Naily, W., (2018). Ratio of major ions in groundwater to determine saltwater intrusion in coastal areas. In *IOP conference series: earth and environmental science* (Vol. 118, No. 1, p. 012021). IOP Publishing.

Nunes, M., (2019). Microalgae as indicators of environmental change in the St Lucia estuarine system., Submitted in fulfilment of the requirements for the degree of Doctor of Philosophy, Nelson Mandela University.

Nunes, M., Adams, J.B. and Bate, G.C., (2019). The use of epilithic diatoms grown on artificial substrata to indicate water quality changes in the lower reaches of the St Lucia Estuary, South Africa. Water SA, 45(1), pp.149-159.

Nunes, M., Adams, J.B. and Rishworth, G.M., (2018). Shifts in phytoplankton community structure in response to hydrological changes in the shallow St Lucia Estuary. Marine pollution bulletin, 128, pp.275-286.

Nunes, M., Adams, J.B., Bate, G.C. and Bornman, T.G., (2017). Abiotic characteristics and microalgal dynamics in South Africa's largest estuarine lake during a wet to dry transitional phase. Estuarine, Coastal and Shelf Science, 198, pp.236-248.

Piper, A.M., (1944). A graphic procedure in the geochemical interpretation of water-analyses. *Eos, Transactions American Geophysical Union*, *25*(6), pp.914-928.

Poeter, E., Fan Y., Cherry, J., Wood, W., and Mackay, D., (2020). Groundwater in our water cycle – getting to know Earth's most important fresh water source, Guelph, Ontario, Canada, p.136

Pulido-Leboeuf, P., (2004). Seawater intrusion and associated processes in a small coastal complex aquifer (Castell de Ferro, Spain). *Applied geochemistry*, *19*(10), pp.1517-1527.

QGIS.org., (2021). QGIS Geographic Information System. QGIS Association. http://www.qgis.org

Rautenbach, C., Barnes, M.A. and de Vos, M., (2019). Tidal characteristics of South Africa. Deep Sea Research Part I: Oceanographic Research Papers, 150, p.103079.

SAEON, (2021). Water level and rainfall data obtained from South African Environmental Observation Network. http://www.saeon.ac.za/

Salem, Z.E.S. and Osman, O.M., (2017). Use of major ions to evaluate the hydrogeochemistry of groundwater influenced by reclamation and seawater intrusion, West Nile Delta, Egypt. *Environmental Science and Pollution Research*, *24*(4), pp.3675-3704.

Salifu, M., Hällström, L., Aiglsperger, T., Mörth, C.M. and Alakangas, L., (2020). A simple model for evaluating isotopic (^{18}O, ^{2}H and $^{87}Sr/^{86}Sr$) mixing calculations of mine–Impacted surface waters. Journal of contaminant hydrology, 232, p.103640.

Schumann, E. H. (1988). Physical oceanography off Natal. In: Coastal Ocean Studies Off Natal, South Africa, Schumann, E. H. (ed.). Berlin: Springer Verlag, pp. 101–130.

Sherif, M.M. and Singh, V.P., (1999). Effect of climate change on sea water intrusion in coastal aquifers. Hydrological processes, 13(8), pp.1277-1287.

Srinivasamoorthy, K., Chidambaram, S., Prasanna, M.V., Vasanthavihar, M., Peter, J. and Anandhan, P., (2008). Identification of major sources controlling groundwater chemistry from a hard rock terrain – a case study from Mettur taluk, Salem district, Tamil Nadu, India. *Journal of Earth System Science*, *117*(1), p.49.

Stretch, D.D. and Maro, A., (2013). Catchment hydrology. Ecology and Conservation of Estuarine Ecosystems: Lake St Lucia as a Global Model. Cambridge University Press, Cambridge, pp.151-167.

Taylor, R., (1991). Greater St. Lucia Wetland Park. Parke-Davis, Cape Town, South Africa, pp.1-50

Taylor, R., Kelbe, B., Haldorsen, S., Botha, G.A., Wejden, B., Været, L. and Simonsen, M.B., (2006). Groundwater-dependent ecology of the shoreline of the subtropical Lake St Lucia estuary. Environmental Geology, 49(4), pp.586-600.

Terzer, S., Wassenaar, L.I., Araguás-Araguás, L.J. and Aggarwal, P.K., (2013). Global isoscapes for δ 18 O and δ 2 H in precipitation: improved prediction using regionalized climatic regression models. *Hydrology and Earth System Sciences*, *17*(11), pp.4713-4728.

Thibault, C.H., (2017). The movement of storm surge through a surficial coastal aquifer (Doctoral dissertation, The University of Memphis).

Torgersen, T., Jenkins, W.J. and Clarke, W.B., (1979). The tritium/helium-3 method in hydrology. In *Isotope hydrology 1978*.

Været, L., Kelbe, B., Haldorsen, S. and Taylor, R.H., (2009). A modelling study of the effects of land management and climatic variations on groundwater inflow to Lake St Lucia, South Africa. Hydrogeology journal, 17(8), p.1949.

Van Wyk, E., (2013). Correlations between rainwater and groundwater geochemistry signatures with reference to episodic rainfall events in semi-arid environments, South Africa. In *The Use of ISOTOPE Hydrology to Characterize and Assess Water Resources in South(ern) Africa*; Abiye, Ed.; WRC: Pretoria, South Africa, 2013; pp. 102–110. 210p.

Vogel, J.C. and van Urk, H. (1975). Isotopic investigation of Lake St Lucia. Unpublished CSIR report

Vrdoljak, S.M. and Hart, R.C., (2007). Groundwater seeps as potentially important refugia for freshwater fishes on the Eastern Shores of Lake St Lucia, KwaZulu-Natal, South Africa. African Journal of Aquatic Science, 32(2), pp.125-132.

Werner, A.D., Bakker, M., Post, V.E., Vandenbohede, A., Lu, C., Ataie-Ashtiani, B., Simmons, C.T. and Barry, D.A., (2013). Seawater intrusion processes, investigation and management: recent advances and future challenges. Advances in Water Resources, 51, pp.3-26.

White, W.M. ed., (2018). *Encyclopedia of Geochemistry: A Comprehensive Reference Source on the Chemistry of the Earth*. Springer International Publishing.

Whitfield, A.K. and Taylor, R.H., (2009). A review of the importance of freshwater inflow to the future conservation of Lake St Lucia. Aquatic Conservation: Marine and Freshwater Ecosystems, 19(7), pp.838-848.

WWF-SA (2016). Water: Facts & Futures, Available at: http://awsassets.wwf.org.za/downloads/wwf009_waterfactsandfutures_report_web__lowres_.pdf

XLSTAT., (2021). Statistical Software for Excel. Available at: https://www.xlstat.com

9. APPENDICES

Appendix A – Sampling points with field data

Sample No.	SAMPLE CODE	LOCATION	LATITUDE	LONGITUDE	pH	EC (µS/cm)	TDS (mg/L)	TEMP (°C)
1	STL-01	St. Lucia town	-28.372255	32.413632	7.04	320	205	23.6
2	STL-02	St. Lucia town	-28.374526	32.412411	6.96	364	233	22.6
3	STL-03	St. Lucia town	-28.376312	32.413606	6.76	304	194.5	22.5
4	KLV-01	Khula Village	-28.365983	32.379397	6.91	388	248	24.9
5	KLV-02	Khula Village	-28.373875	32.379731	5.57	365	234	23.1
6	KLV-03	Khula Village	-28.370463	32.380523	7.02	618	396	23.9
7	KLV-04	Khula Village	-28.373611	32.368033	5.39	346	222	23.6
8	KLV-05	Khula Village	-28.378838	32.361947	7.46	470	301	26.5
9	KLV-06	Khula Village	-28.378288	32.361176	7.04	257	164.6	25.7
10	KLV-07	Khula Village	-28.378652	32.359757	6.26	529	339	25.9
11	KLV-08	Khula Village	-28.376480	32.369916	5.76	751	481	24.4
12	KLV-09	Khula Village	-28.375003	32.370730	6.5	393	251	25.5
13	KLV-10	Khula Village	-28.364379	32.369906	6.73	317	203	26.3
14	KLV-11	Khula Village	-28.357212	32.374062	5.58	320	205	26.9
15	KLV-12	Khula Village	-28.361926	32.372425	6.3	235	150.7	30.3
16	KLV-13	Khula Village	-28.363496	32.375475	7.56	208	132.9	28.1
17	KLV-14	Khula Village	-28.364384	32.377021	8.05	314	201	27.3
18	KLV-15	Khula Village	-28.364023	32.379444	7.2	299	191.5	32.8
19	KLV-16	Khula Village	-28.361734	32.380313	6.45	451	289	24.3
20	KLV-17	Khula Village	-28.379101	32.365260	7.22	602	385	24.4
21	DKV-01	Duku Village	-28.376438	32.378780	6.29	242	154.6	25.3
22	DKV-02	Duku Village	-28.377040	32.385357	7.48	422	270	29.4
23	DKV-03	Duku Village	-28.376581	32.378059	5.41	363	232	28.5
24	DKV-04	Duku Village	-28.378964	32.376741	7.09	178.7	114.4	27.4
25	DKV-05	Duku Village	-28.380677	32.363809	5.96	397	254	26.1
26	DKV-06	Duku Village	-28.381104	32.363813	5.76	321	205	28.9
27	DKV-07	Duku Village	-28.384651	32.362879	5.18	572	366	25.2
28	DKV-08	Duku Village	-28.388907	32.364534	5.81	868	555	27.5
29	DKV-09	Duku Village	-28.383201	32.363697	5.35	362	232	27
30	KLV-18	Khula Village	-28.379236	32.362959	5.47	496	317	26.1
31	KLV-19	Khula Village	-28.380045	32.362490	5.43	270	173.1	23.3
32	KLV-20	Khula Village	-28.384558	32.349800	7.29	446	285	27.3
33	STL-04	Manzini Chalets	-28.378742	32.409668	5.97	396	253	29.2
34	STL-05	Backpackers' accommodation	-28.376454	32.411315	6.67	349	223	24.6
35	STL-06	Ski Club	-28.383720	32.418037	7.39	9260	5930	24.4
36	EST-01	estuary Sunset Jetty	-28.379398	32.407670	6.94	290	185.6	25.9

37	OCN-01	ocean cape vidal	-28.125185	32.557854	8.04	59900	38300	27.5
38	EST-02	estuary boardwalk	-28.380923	32.422002	7.08	1886	1207	25.6
39	EST-03	estuary mouth low tide	-28.385845	32.424065	7.33	791	506	25.6
40	STL-07	st lucia security	-28.374802	32.419854	7.28	248	158.8	27.1
41	STL-08	avalone	-28.375894	32.419377	7.01	387	248	25.5
42	STL-09	st lucia construction	-28.375354	32.418103	7.53	290	185.5	26.4
43	STL-10	st lucia heidi	-28.376474	32.418472	6.6	538	344	27.4
44	STL-11	hilltop 19m water @7m	-28.374985	32.417756	6.54	273	174.6	23.1
45	STL-12	guesthouse ocean view	-28.382314	32.413070	6.14	347	222	23
46	UMF-01	river mfolozi	-28.467347	32.295720	6.92	186.6	119.4	23.7
47	EST-04	estuary cruise 1	-28.368284	32.410784	7.64	185.1	116.5	24.5
48	EST-05	estuary cruise 2	-28.360556	32.407711	7.29	182.6	116.9	24.3
49	EST-06	estuary cruise 3	-28.326561	32.405712	7.2	203	130.1	24.6
50	OCN-02	ocean beach	-28.384722	32.425763	7.21	5430	3470	26.7
51	OCN-03	ocean wave dancer	-28.388877	32.436351	7.88	60500	38700	26.8

Appendix B – δ^2H (‰) values for all samples

Sample name	**δ^2H (‰)**	**± ^2H St Dev (‰)**
STL-01	-22.2	4.3
STL-02	-14.8	0.2
STL-03	-15.9	0.3
KLV-01	-13.0	0.4
KLV-02	-19.5	0.3
KLV-03	-18.5	0.6
KLV-04	-16.0	0.2
KLV-05	-15.9	0.2
KLV-06	-15.8	0.3
KLV-07	-16.6	0.1
KLV-08	-19.0	1.1
KLV-09	-9.6	0.5
KLV-10	-15.7	0.2
KLV-11	-18.3	0.2
KLV-12	-18.7	0.2
KLV-13	-19.4	2.6
KLV-14	-18.0	0.2
KLV-15	-17.4	0.1

KLV-16	-16.7	0.2
KLV-17	-15.7	0.3
DKV-01	-20.2	3.5
DKV-02	-10.3	0.4
DKV-03	-13.9	0.4
DKV-04	-17.8	0.4
DKV-05	-18.0	0.3
DKV-06	-24.3	4.7
DKV-07	-21.1	0.2
DKV-08	-23.4	0.3
DKV-09	-11.4	0.7
KLV-18	-16.7	0.4
KLV-19	-21.6	0.7
KLV-20	-6.5	0.6
STL-04	-18.1	0.7
STL-05	-15.5	0.2
STL-06	-11.1	0.3
EST-01	-21.1	1.0
EST-02	-34.6	0.5
EST-03	-37.4	0.3
STL-07	-18.5	0.5
STL-08	-15.7	0.2
STL-09	-16.4	2.3
STL-10	-15.4	0.1
STL-11	-15.6	0.2
STL-12	-16.6	0.4
UMF-01	-41.0	0.9
EST-04	-45.0	2.6
EST-05	-42.8	0.3
EST-06	-37.6	0.3
OCN-02	-38.1	0.2
DI	-14.3	0.6
OCN-03	-7.1	5.4
OCN-01	-3.3	0.1
DI	-14.3	1.0

Appendix C - $\delta^{18}O$ (‰) values for all samples

Sample name	**$\delta^{18}O$ (‰)**	**± ^{18}O St Dev (‰)**
STL-01	-5.41	0.3
STL-02	-4.62	0.1
STL-03	-4.64	0.1
KLV-01	-3.80	0.1
KLV-02	-5.30	0.1
KLV-03	-5.30	0.1
KLV-04	-4.82	0.1
KLV-05	-4.32	0.0
KLV-06	-4.28	0.1
KLV-07	-4.50	0.0
KLV-08	-5.05	0.1
KLV-09	-2.99	0.1
KLV-10	-4.58	0.1
KLV-11	-4.89	0.0
KLV-12	-4.89	0.0
KLV-13	-4.96	0.2
KLV-14	-4.93	0.1
KLV-15	-4.94	0.0
KLV-16	-4.86	0.1
KLV-17	-4.35	0.1
DKV-01	-5.07	0.2
DKV-02	-2.53	0.1
DKV-03	-4.36	0.0
DKV-04	-4.31	0.1
DKV-05	-4.81	0.0
DKV-06	-5.66	0.4
DKV-07	-5.47	0.1
DKV-08	-5.77	0.1
DKV-09	-3.27	0.1
KLV-18	-4.84	0.1
KLV-19	-5.54	0.0
KLV-20	-1.82	0.1
STL-04	-5.29	0.1
STL-05	-4.59	0.1
STL-06	-3.88	0.1
EST-01	-4.94	0.1
EST-02	-6.61	0.0
EST-03	-7.28	0.1
STL-07	-5.39	0.1
STL-08	-4.67	0.0
STL-09	-4.98	0.3

STL-10	-4.66	0.0
STL-11	-4.83	0.0
STL-12	-4.79	0.1
UMF-01	-7.57	0.1
EST-04	-7.93	0.2
EST-05	-7.80	0.0
EST-06	-6.93	0.0
OCN-02	-7.07	0.0
DI	-3.40	0.1
OCN-03	-1.35	0.4
OCN-01	-1.25	0.1
DI	-3.32	0.1